PREPARATION AND EVALUATION OF NICKEL BASED METALLIC GLASS BRAZING FOILS

A thesis submitted
in Partial Fulfilment of the Requirements
for the degree of

MASTER OF TECHNOLOGY

by

SUMITA CHAKLANOBIS

to the

INTERDISCIPLINARY PROGRAMME IN METERIALS SCIENCE
INDIAN INSTITUTE OF TECHNOLOGY, KANPUR

AUGUST, 1984

C E R T I F I C A T E

This is to certify that this thesis entitled 'Preparation and Evaluation of Nickel Based Metallic Glass Brazing Foils' submitted in partial fulfilment of the requirements for the Degree of Master of Technology by Ms. Sumita Chaklanobis. is a record of work carried out under my supervision and has not been submitted elsewhere for a degree.

D.C. Agrawal
Assistant Professor
Materials Science Program
Indian Institute of Technology
Kanpur- 208016

ACKNOWLEDGEMENT

I,

am extremely thankful to Dr. D.C. Agrawal for his valuable guidance and tolerance throughout this work.

owe my entire work output to my parents for their blessings and continuous encouragement.

express my gratitude to Mr. D.B. Chakraborty for rendering all possible assistance when-ever needed.

acknowledge the good humour and assistance of Shilpi and the help given by Sujata.

thank Mr. H.C. Bhattacharyya, Mr. A.K. Ganguli, Mr. B.D. Biswas, Mr. S. Das, and Mr. Viswanath for their valuable contributions.

gratefully acknowledge the service of Central Work-shop, Glass Blowing Section and Graphic Arts Section.

sincerely thank the faculty and staff of A.C.M.S. and Metallurgy for their ever ready help as and when required.

also thank all my friends for their help and co-operation.

I.I.T. Kanpur

SUMITA CHAKLANOBIS

August, 1984

CONTENTS

LIST OF FIGURES

ABSTRACT

Of the many potential applications of metallic glasses, one relatively small scale but important application is as brazing foils. The application becomes attractive for nickel base alloys used for brazing stainless steels because while these alloys are brittle in the crystalline state and can be used only in powder form, the rapidly solidified foils of the same compositions are ductile and can be punched to desired shapes, thus leading to the possibility of using preforms, more accurate metering and absence of binders.

In the present work the brazing characterstics of some nickel based metallic glass brazing foils have been studied. The wide ductile metallic glass ribbons required for the brazing process to serve as brazing foils were prepared after establishing the preparation conditions for such foils using aluminium. A standard brazing composition BNi-4 as well as it's two variations with different iron contents were used for the investigations. Two halves of the tensile test specimens of 304 stainless steel were brazed using these foils. Brazing conditions for maximum joint strength were established. The tensile strength, ductility, microstructure and microhardness across the joint were studied. The tensile strength of the joints increase with the increasing iron content. The strength

is comparable to that obtained by other investigators with similar foils as well as with common silver brazing alloy. The ductility increases with increasing iron content. The width of the brazed zone also increases as iron content increases. Peaks in microhardness across the brazed zone are obtained which could be due to composition variation.

CHAPTER I

INTRODUCTION

I.1 THE METALLIC GLASSES

The term metallic glass refers to amorphous metallic alloys which are obtained by rapid cooling of the melt. The cooling rates required for the formation of metallic glasses are of the order of $10^6 {}^oK.s^{-1}$. Although several techniques are capable of producing amorphous alloys[1-5], the melt spinning technique developed in 1908[6] after certain modifications[7], has been found to be the most suitable one for the continuous production of amorphous alloy ribbons or the metallic glass ribbons. The rapid quenching of the melt of the corresponding alloy through the temperatures at which the normal solidification occurs results in the retainment of a liquid like structure in the solid, instead of solidification by normal crystallization. The metallic melts have non-directional bonding and the atomic rearrangement process is very rapid even when the degree of under-cooling is far bellow that of their equilibrium freezing temperatures. Appreciable amount of atomic diffusion is prevented in the rapid cooling process and the nucleation and subsequent growth of the equilibrium structures are inhibited. The increased atomic mobility in the liquids as compared to that in solids, require the imposition of much higher cooling rates to bypass crystallization as compared to those required to avoid solid state transformations.

The required cooling rate ($\geq 10^6$ K/s) to obtain metallic glass phase, was first achieved by Klement, Willens and Dewez in 1960[8], when they developed the splat cooling technique which involved the continuous cooling from the melt.

Development from the laboratory to real life applications of rapidly quenched alloys can be attributed to their attractive engineering charecterstics such as soft magnetic properties[9], high mechanical strength[10] and extremely high corrosion resistance, which are superior to those of their crystalline counterparts. High magnetostriction and low acoustic losses enables them to be used in transducers, load cells, length measuring devices etc. Soft magnetic property and low core losses are the appropriate properties for their application in transformers, electric motors, choke coils etc. and high permeability makes them a suitable choice for use in magnetic recording heads and magnetic sheilding. Also the various potential applications of these metallic glasses are for tire cords and composite materials, rraterials coated with amorphous alloys for corrosion resistance, powder or their compacted products for catalysts, gas absorbers and ion adhesion materials, electrodes for fuel cells etc. in the near future. Recently metallic glass foils are finding increased applications in the production of high strength metal joints by brazing, and are fast replacing the conventional brazing filler foils or brittle powders held in organic bounders[13].

I.2 BRAZING AND BRAZING FILLER METALS FOR STAINLESS STEEL

Brazing includes a group of processes which produce bonding of materials by heating them to a suitable temperature using a filler material having a liquidus above 426.6°C (800°F) and below the solidus of the material being joined. Brazing fuses the base metals by creating a metallurgical bond at the molecular level between the filler metal and the surfaces of the base metal being joined. The process involves wetting of the surfaces being joined by the molten filler material and the subsequent filling of the joint spaces by capillary penentration due to surface tension forces.

Filler metals should be judged for their ability to resist corrosion and oxidation, their remelt temperature, and their flowability and whether they diffuse readily or not etc. Compositions of fillers become important when the brazement is to be subjected to chemically corrosive or high temperature service conditions. It must resist chemical corrosion and must not remelt at the service temperature of the brazement. If the brazement is to be subjected to high temperature service conditions, it must have sufficient strength to prevent creep and to with-stand thermally and mechanically induced stresses and plastic deformation at the service temperatures. The degree of diffusibility must be matched to the application. A highly diffusible brazing alloy may seriously erode the base metal ajecent to the

joint and would thus prove unusable for use in an assembly employing thin sections (eg. honey comb structures). In another application, the same diffusing type of filler material may be desirable to attain a high enough remelt temperature.

Silver based brazing alloys (Ag - Cu eutectic alloys modified by addition of znic, cadmium, tin, mangnese, nickel etc.) are the prime filler materials for stainless steel brazing. Copper based fillers (with znic and nickel) are also in use. High temperature steel brazing alloys are palladium bearing (Pd - Ni, Pd - Ag, Pd - Cu) and gold based (with copper, nickel, palladium) alloys. (See appendix) Nickel based series of fillers covering a wide range of compositions have been developed in general for heat and corrosion resistance, in certain of the most stringent service applications for brazing stainless steel. Table I presents a list of the nickel based fillers in use for brazing stainless steel[14]. Carbon and low alloy steels are also sometimes joined with these alloys where for example better corrosion resistance is required compared to those using copper based fillers, but they find their widest application in the brazing of stainless steel assemblies. Some of these fillers retain good strength upto nearly 1000°C or are also satisfactory at cryogenic temperatures.

Good high temperature resistance makes nickel a good starting point in the development of filler metals for high temperature service. Proper addition of other elements produce filler

TABLE I

NICKEL BASED COMPOSITIONS FOR STAINLESS STEEL BRAZING

SPECIFICATIONS AWS	NOMINAL COMPOSITIONS pct,	MELTING POINT (°C) SOLIDUS	MELTING POINT (°C) LIQUIDUS	BRAZING RANGE (°C)	FILLER METAL DESCRIPTION
B Ni -1	13-15 Cr, 2.75-4B, 3-5 Si, 4-5 Fe, Bal Ni	970	1040	1065 - 1205	Widely used for well diffused, high strengh, heat resistant joints. For highly stressed structures, such as jet engine parts
B Ni -2	6-8 Cr, 2.75-3.5B, 4-5 Si, 2-4 Fe, Bal Ni	970	1000	1010 - 1175	Properties and uses are similar to B Ni-1 except that it can be brazed at lower temperatures
B Ni -3	2.75-3.5B, 4-5 Si, 1.5 Fe, Bal Ni	980	1040	1010 - 1175	A good general purpose filler metal, it flows freely in marginal atmospheres, in deep or tight joints. Applications similar to B Ni-1
B Ni -4	1-2.2B, 3-4 Si, 1-5 Fe, Bal Ni	990	1055	1065 - 1180	Combines the properties of wide melting range, free flowing properties, machinability and low diffusion with most base metals

Table I (Cont.)

ECIFICATIONS AWS	NOMINAL COMPOSITIONS pct.	MELTING POINT (°C) SOLIDUS	LIQUIDUS	BRAZING RANGE (°C)	FILLER METAL DESCRIPTION
B Ni -5	18-20 Cr, 9.75-10.5 Si, Bal Ni	1080	1135	1150 - 1205	For uses similar to B Ni -1, plus nuclear reactor uses where boron can not be used. High strength with low base metal penentration
B Ni -6	10-12 P, Bal Ni	875	875	925 - 1095	A free flowing, low melting, chromium free filler metal, good for marginal atmospheres. Minimises base metal erosion
B Ni -7	11-15 Cr, 9-11 P, Bal Ni	890	890	980 - 1095	A low-melting, free flowing filler metal for honey-comb structures and thin walled tube assemblies. Has low solubilities
	SOME COMMERCIALLY AVAILABLE FILLER METALS				
ICROBRAZ 51	25.0 Cr, 10.0 P, Bal Ni				Similar to B Ni -7 except for better strength, heat and corrosion resistance

SPECIFICATIONS AWS	NOMINAL COMPOSITIONS pct.	MELTING POINT (°C) SOLIDUS	LIQUIDUS	BRAZING RANGE (°C)	FILLER METAL DESCRIPTION
NICROBRAZ 150	15.0 Cr, 3.5 B, Bal Ni	1055	1055	1065 - 1205	Excellent for jet engine parts and similar highly stressed components. Good strength at lower brazing temperatures than B Ni -1 or B Ni -5
NICROBRAZ 160	11.0 Cr, 3.5 Fe, 2.25 B, 0.5 C, 3.5 Si, Bal Ni	970	1160	1170 - 1205	For wide clearance joints where heavier fillets or greater joint ductility and machinibility are desired
NICROBRAZ 170	12.0 Cr, 3.5 Fe, 2.5 B, 16.0 W, 3.5 Si, 0.5 C, Bal Ni	970	1105	1150 - 1205	For use where extra high strength at high temperatures is required. Good for brazing base metal containing cobalt, tungsten and molybdenum
NICROBRAZ 171	10.0 Cr, 3.5 Fe, 2.5 B, 12.0 W, 3.5 Si, 0.4 C, Bal Ni	970	1095	1150 - 1205	Applications similar to Nicrobraz 170 except for better flow
NICROBRAZ 200	7.0 Cr, 6.0 W, 4.5 Si, 3.0 Fe, 3.2 B, Bal Ni	975	1040	1065 - 1175	Recomended for components where hardenable base metals are used. High creep and stress rupture strengh

NICROBRAZ - Registered U.S Patent

metals having excellent strength and oxidation resistance as well as high temperature corrosion resistance. It has been found that Ni - Fe alloys appear to have better corrosion resistance than nickel alloys[15]. When used as brazing fillers in ammonia water and also display required capillarity, filleting and wetting. Silicon and boron are usually added as melting point depressors. These have virtually no solubility in solid nickel and thus the silicides and borides which are present in significant volume fractions, make polycrystalline solid extremely brittle and difficult to fabricate into thin shapes conducive to brazing. On the other hand, the use of powder fillers along with organic binders pose their own difficulty of causing shrinkage of the joint when the baking off of the binders is done and it also leaves behind contaminating residues. Also since powder fillers in the paste form if used, are applied to the joint edge and capillary action draws the filler material to cover the mating surfaces, hence they are not suitable for brazing wide and deep joints. Joint spacers to provide uniform gap between the mating surfaces also have to be used while using powder fillers.

I.3 METALLIC GLASS BRAZING FOILS

Recently it has been found that several nickel based brazing filler compositions which are brittle and can be used only as powders when made by the conventional methods, can be rapidly quenched from the liquid state to produce ductile foils and

this simplifies many aspects of brazing operation[13]. They also offer technological advantages as melt quenching technique is a simplified production process with high productivity. Such metallic glass ribbons can be bent to match with complex joint geometrics. They can also be punched to the exact joint shapes. They can be produced in thicknesses corresponding to maximum joint strength and metering of these ductile foils is also more easy than their powder counterparts. These metallic glass foils are 100 pct. dense and binders of any sort are not required as is the case in using powder fillers. The advantage of the ductility of these foils which is due to it's amorphous nature is used in placing it at the joint and the fact that they become crystalline during the heating cycle of the brazing operation is of no detriment.

The conventional high temperature gold based filler are currently being replaced by the nickel based ductile brazing foils and this is primarily because of economic reasons[16]. Also like the gold based fillers, these nickel based foils have been found to have excellent flow behaviour, compatibility with most stainless steels and offer an outstanding combination of high temperature strength, fatigue properties and oxidation resistance. The ductilities are also comparable and the base metal pitting is also less severe as compared to the brazements using gold based fillers. Above studies have been done with BNi - 1,

BNi -2, BNi -3 and BNi -6 brazing foils to compare their properties with those of the conventional noble metal based filler alloys. The use of nickel based foils (BNi -1..) in brazing jet engine parts results in cost reduction and improved strength[1 A 60 pct. increase in strength, sulphur oxidation resistance an better production economics, as compared to the formerly used brazing alloys is obtained. The nickel based fillers for brazin have also been tested and have been found to cut cost and conta mination in food industry[18]. It reduces scrap loses and fille metal cost by switching from silver to nickel based brazing fil lers in brazing carbonated beverage can filling equipments and also meets the FDA regulations banning cadmium (used in silver based alloys as melting point depressors).

I.4 PRESENT WORK

The rapidly increasing use of the nickel based amor phous foils as brazing filler materials in various industrial applications has motivated us into preparation and determinatio of the suitability of the metallic glass brazing foils. A standard composition BNi -4 (See Table I) was chosen and its iron content was varied and the effect on the resulting brazements was studied. For this we required amorphous foils wide enough to cover the mating surfaces to be joined. In the subsequent chapters first the preparation of the wide metallic glass ribb is described followed by their application in the brazing of commercial stainless steel.

CHAPTER II

PREPARATION OF WIDE METALLIC GLASS RIBBONS

II.1 INTRODUCTION

The various effects of rapid solidification of alloys from the corresponding melt namely, structural, morphological and constitutional are now pretty well established[19-21]. These cause refinement of microstructure, enhanced supersaturation of vaccancies and of solute elements and complete or partial avoidance of crystallization, thus forming metallic glass. High cooling rates,($\geq 10^6$ K s^{-1}) are generally required for metallic glass formation and these cooling rates can be achieved in thin melt sections which are in good thermal contact with an effective heat sink[22]. Thus most rapid quenching techniques are based on the fundamental requirement of bringing the melt into contact with a cold and highly conducting substrate at high relative velocity to promote melt spreading and thereby forming thin sections and intimate thermal contact. For the begining of crystallization, an undercooling of the liquid bellow the equilibrium crystallization temperature is necessary due to the exsistence of an energy barrier to the formation of nuclei[22-25]. But if the liquid is cooled rapidly by removing the heat to a sink as described above, the undercooling is enhanced and thus the temperature range over which the process

of crystallization occurs is greatly reduced. This leads to structural modifications and refinement of microstructure and eventually at sufficiently high cooling rates, complete suppression of crystallization because of insufficient time for sufficient growth (microcrystalline) or in the extreme case for nucleation (amorphous). The atomic configuration of metallic glasses have been found by the analysis of diffraction data, to bear a close resemblence to the static equilibrium liquid structure near its freezing temperature, but the glass atoms vibrate about positions which are more condensed. The local structure in metallic glasses is that of the derivative inter-metallic crystalline phase with the structural units essentially disordered which is similar to the network in glass.

II.2 CHILL BLOCK MELT SPINNING

In the recent years a continuous melt spinning technique, namely chill block melt spinning (CBMS) has been evolved to produce metallic glass ribbons. It is derived from the origional patented technique of Pond[26] and involves the impingement of a molten metal jet onto a moving cold substrate. Furthur it also meets the requirement of the formation of filaments, sufficiently thin so that the cooling rate exceeds the critical cooling rate for glass formation and also the contact between the filament and the substrate (heat sink)

is of sufficient duration to lower the temperature well below the nose of the C-C-T curve (Figure II.1).

In this process a melt puddle is formed at the foot of the impinging jet of the molten metal on the substrate, and this puddle spreads and governs the dimensions of the resultant ribbon in accordance to the law of mass balence[27]. The width of the puddle determines the ribbon width and the thickness of the ribbon is dictated by the length of the melt puddle. Several empirical relations between Q, the melt flow rate ; Vs, surface velocity of the substrate; P, ejection pressure and the ribbon dimensions (width, w and thickness, t) have been reported[28-30]. Many experimentally observed data have also been reported to fit empirical relations like

$$t \alpha \; Q^{A}, \; V^{-B}, \; \theta^{m}$$

where θ is the contact time and A, B and m are geometric coifficients. Table II [31] presents these empirical relationships.

To derive these functional relationships initially the total mass balence equation must be considered.

$$Q = t.w.Vs$$

Then we must assume that the ribbon width equals the puddle width and the ribbon thickness is related to the puddle length as

$$t \alpha \left(\frac{1}{Vs}\right)^{m}$$

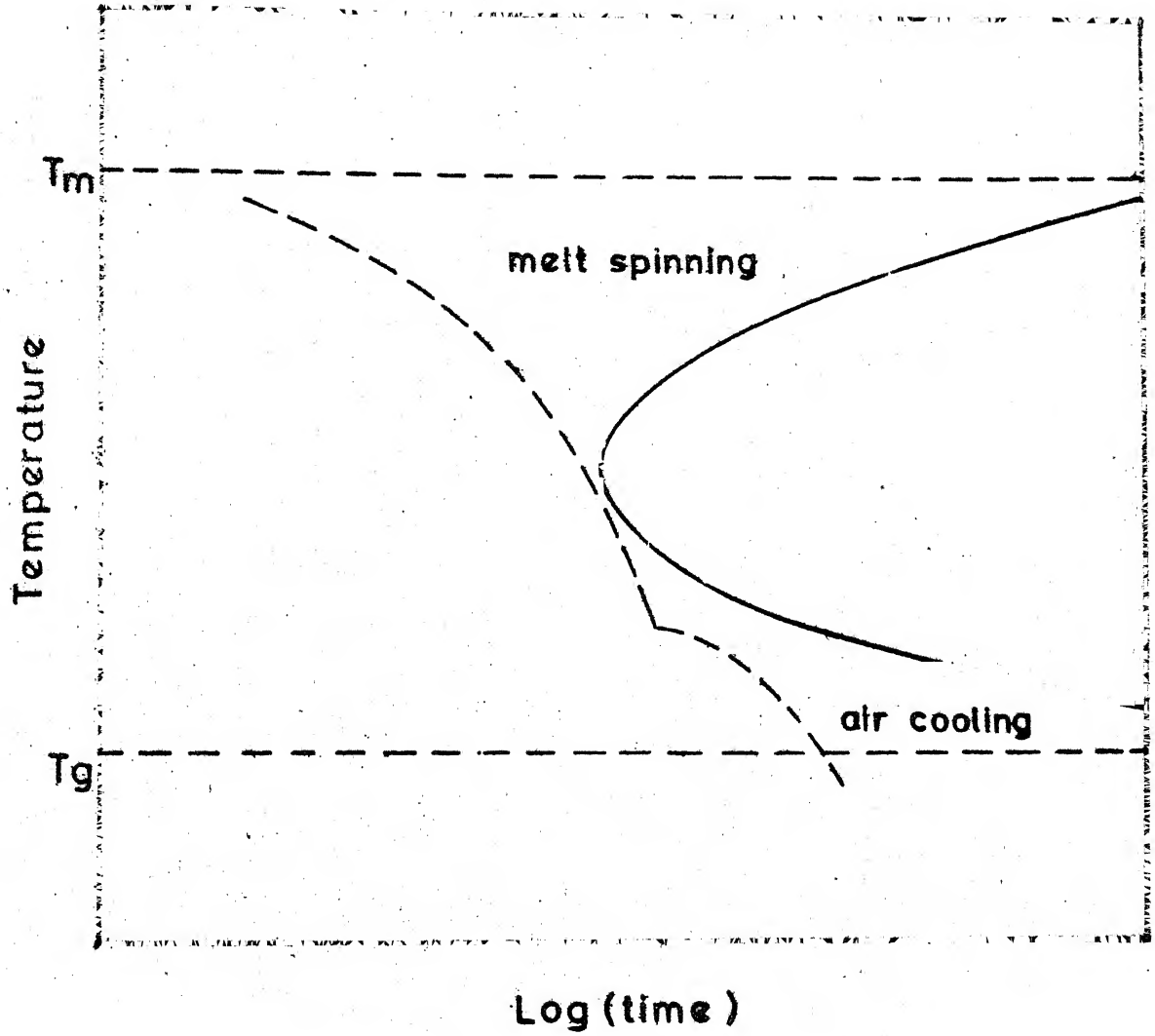

Fig. II.1 Schematic showing the minimum cooling rate required for glass formation in relation to the C-C-T curve of a glass forming alloy

Table II

EMPIRICAL RELATIONSHIPS BETWEEN t,Q,Vs,θ

MATERIAL	STRUCTURE	A	B	m
$Fe_{40}Ni_{40}B_{20}$	amorph.	0.35	0.9	-
Pb Sn eutectic	cryst.	0.19	0.81	-
Al (Fe,Mn)	cryst.	0.25	0.75	-
Waspalloy	cryst.	-	0.73	-
Al-$Si_{10.5}$	cryst.	-	0.76	-
Cu Zn solder	cryst.	-	0.67	-
$Fe_{80}P_{13}C_7$	amorph.	-	0.75	-
$Fe_{40}Ni_{40}P_{14}B_6$	amorph.	0.17	0.83	-
$Fe_{40}Ni_{40}P_{14}B_6$	amorph.	-	-	0.53
$Fe_{81.5}B_{14.5}Si_4$	amorph.	-	-	0.5
$Fe_{80}P_{13}C_7$	amorph.	-	0.93	0.73

(Reference 31)

And lastly, the assumption that the puddle spreads as a circle or ellipse and expands in proportion to the dimensions of it's axis,

or, $\frac{l}{w}$ = constant

One can show that on the basis of these three basic assumptions, the results equivalent to those derived on the basis of several proposed models[30] can be obtained. They are

$$t \alpha \frac{Q^n}{Vs^{2n}}$$

$$w \alpha \frac{Q^{1-n}}{Vs^{1-2n}}$$

where, $n = \frac{m}{1+m}$

Similar results (consistent with the empirical relations) as obtained employing just the basic assumptions are also obtained using the various theoritical models put forth to explain the ribbon formation mechanism, the thermal transport controlling mechanism and the momentum transport controlling mechanism[30].

The ribbon width is found to be strongly dependent on the melt flow rate, Q and the thickness, on the substrate surface velocity, Vs[33]. The pressure dependence of the ribbon thickness was found experimentally and Figure II.2[34] and Figure II.3[35] show the results obtained by two workers. According to Huang[34], the thickness increases initially with

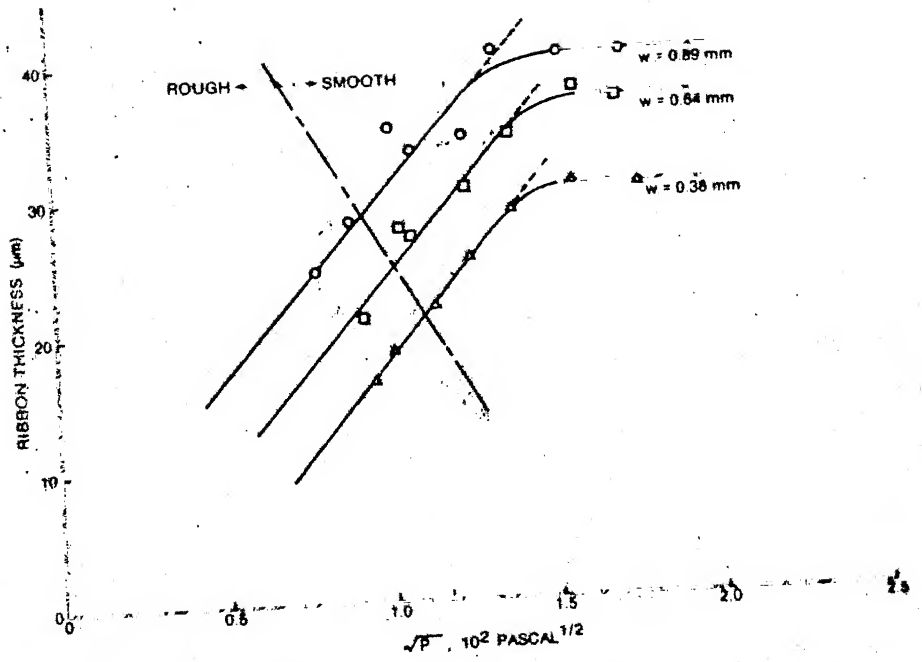

Fig. II.2 Ribbon thickness vs. square-root of the ejection pressure measured at three different slot widths, w (Ref. 34)

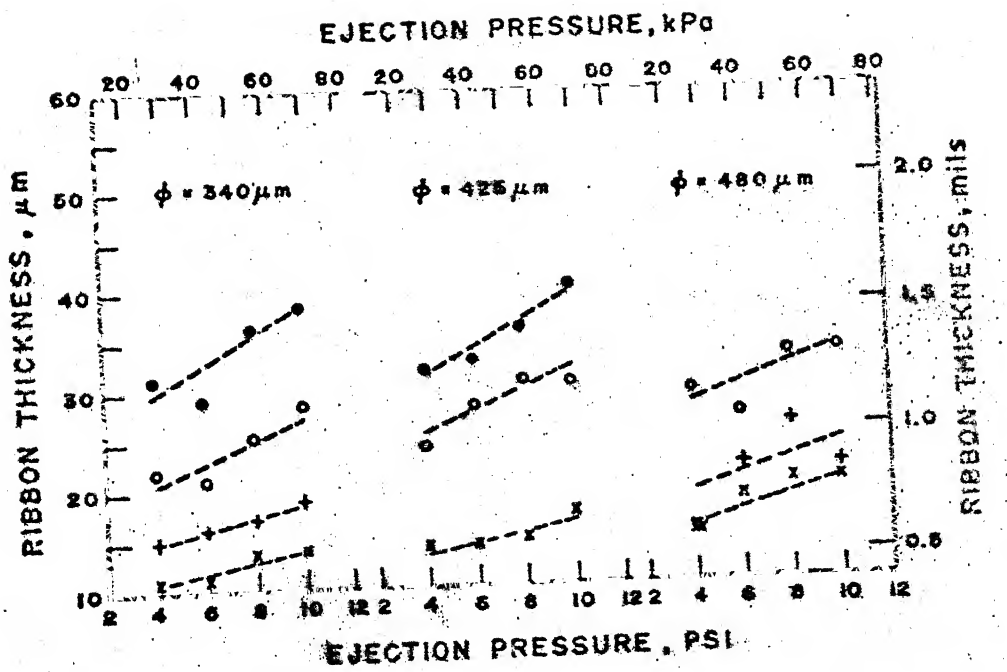

Fig. II.3 Variation of ribbon thickness with ~~disc~~ speed, melt ejection pressure and crucible orifice diameter for glassy $Fe_{40}Ni_{40}B_{20}$ alloy (Ref. 35)

the increase in pressure and at higher pressures (above $\not{\emptyset}$ $\not{\approx}$ 2 x 10^4 Pa), saturates to a fixed value of $t_{max.}$. On the other hand, according to Graham and Liebermann[35] the thickness is governed by Vs but the effect of pressure is also not negligible (for pressures above 2 x 10^4 Pa). Increasing P at constant Vs increases t. The width, w was found to be varing with the crucible orifice diameter $\emptyset$. The process variables, pressure,P and substrate surface velocity, Vs also influence the ribbon surface finish[34]. Wetting patterns at high pressure cast ribbons have small air pockets, irregular in shape and uniform in distribution,replicating the geometry of the wheel surface. As the pressure is reduced, larger air pockets develop through elongation in casting direction.

The CBMS technique involves the melting of the alloy in a crucible and ejection of the molten alloy through a small orifice by appling gas pressure. The ejected jet of the molten metal then impinges on the surface of a rapidly rotating wheel and a continuous ribbon is formed by quenching and the ribbon is finally detached from the wheel by centrifugal forces. This produces the required cooling rate for metallic glass formation (above 10^6°K s^{-1}) for most alloys and a continuous production of amorphous ribbons at a rate of 20 - 50 m s^{-1} is achieved.

II.3 PLANAR FLOW CASTING

Process development for the fabrication of metallic glass ribbons wider than the typical few millimeters as obtained by the CBMS technique requires an elongated molten alloy reservoir which is transversely maintained above the moving substrate surface, to obtain a planar flow of the molten alloy[36,37]. One method used to melt spin wider ribbons involves the use of an array of round jets streaming from the melt ejection crucible and impinging in a transverse line across the moving substrate, thereby forming a broad melt puddle from which wide ribbon is cast. An alternative approch is to use a crucible with a slit shaped orifice in order to impinge a planar molten alloy jet onto the moving substrate surface for making wide ribbons[38]. However, stream geometry destabilization caused by high surface tension and low viscosity of the molten alloys pose difficulties in the use of planar melt jet. To overcome this difficulty, the nozzle which feeds the molten alloy is held very close to the moving substrate surface thus substantially reducing the purturbation of the melt on the substrate by the gas boundary layer, substrate surface roughness etc. This is because the melt is mechanically constrained by the crucible nozzle walls as shown in Figure II.4[40]. In this process the nozzle substrate geometry can be extended

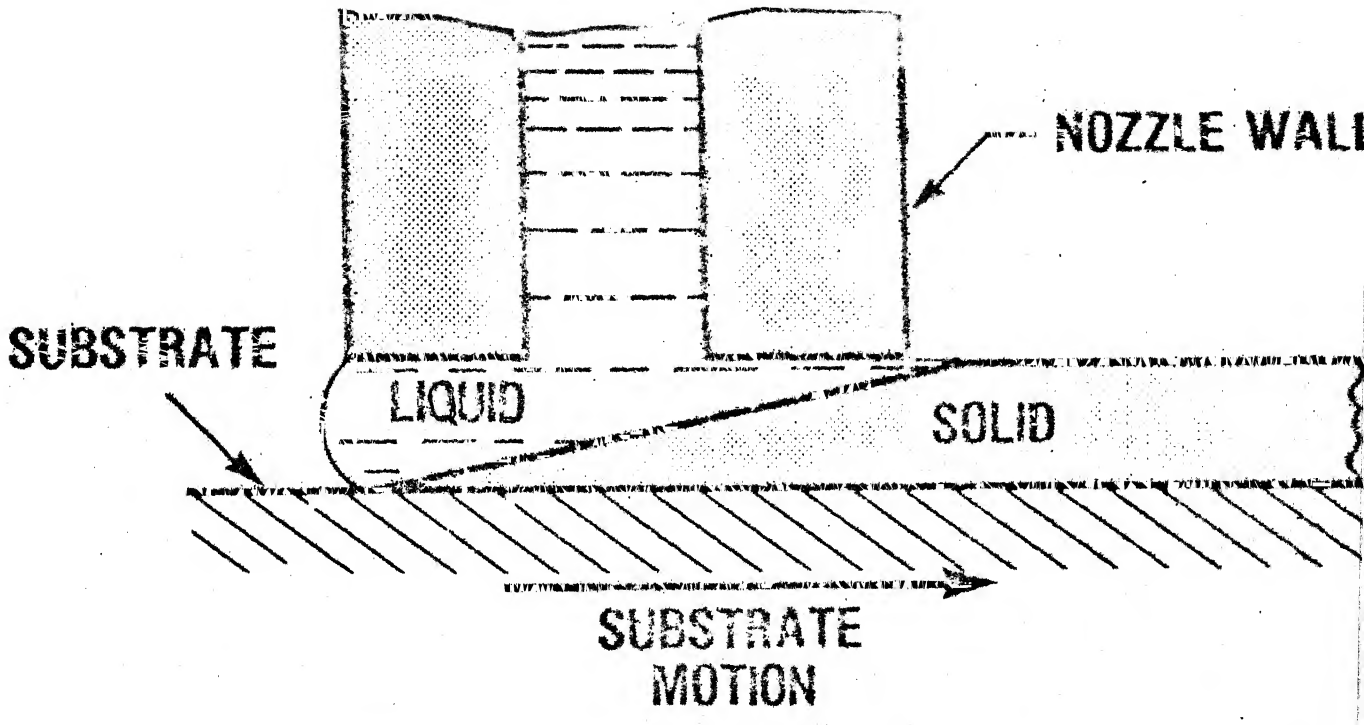

Fig. II.4 Schematic side view of nozzle-substrate geometry in planar flow casting (After Narashimhan[36], taken from Ref.40)

indefinately thereby allowing the production of wide ribbons. Emperical relations for the planar flow casting process for fabrication of wide ribbons have been put forth[36,39] and are similar to those for the CBMS process.

II.4 EXPERIMENTAL

II.4.1 PREPARATION OF SLIT ORIFICE NOZZLE

The crucibles and the nozzles used for melting and spinning were made of clear fused silica tubes. For this purpose 10 mm internal diameter tubings were used. The tubes were cut to approx.20 cm length, closed at one end and the closed end was blown in cavities carved out in graphite peices so as to get rectangular shape at the end of gradually tapered nozzle as shown in Figure II.5(a) to Figure II.5(d). The objective sought to be achieved by this technique was to get reproducible contours of the nozzle section. However it was found that this contour also depended on the temperature to which the silica tube was preheated before blowing and the workmanship of the glass blower during the blowing process. However, the nozzle profiles were more reproducible than could be achieved by just pressing the softened end of the tube. The nozzles thus shaped were then carefully ground so as to get a flat lower end and a slit on the ground surface was cut by a Microslice -2 precision saw. The tube was held on a sliding fixture, pressing the closed end against the saw blade(78 mm diameter). Different slit sizes were obtained by varing the depth of the cut.

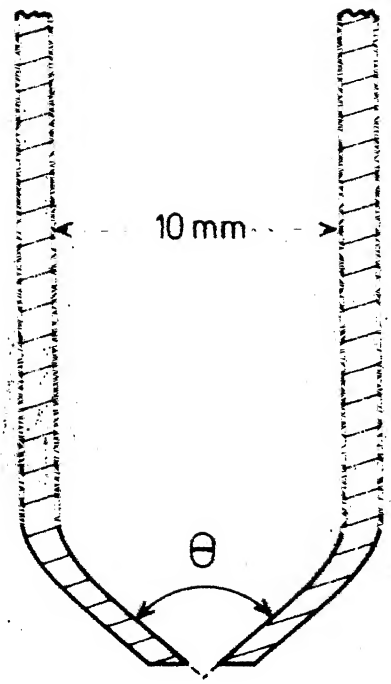

Fig. II.5(a) Schematic defining the nozzle angle, θ.

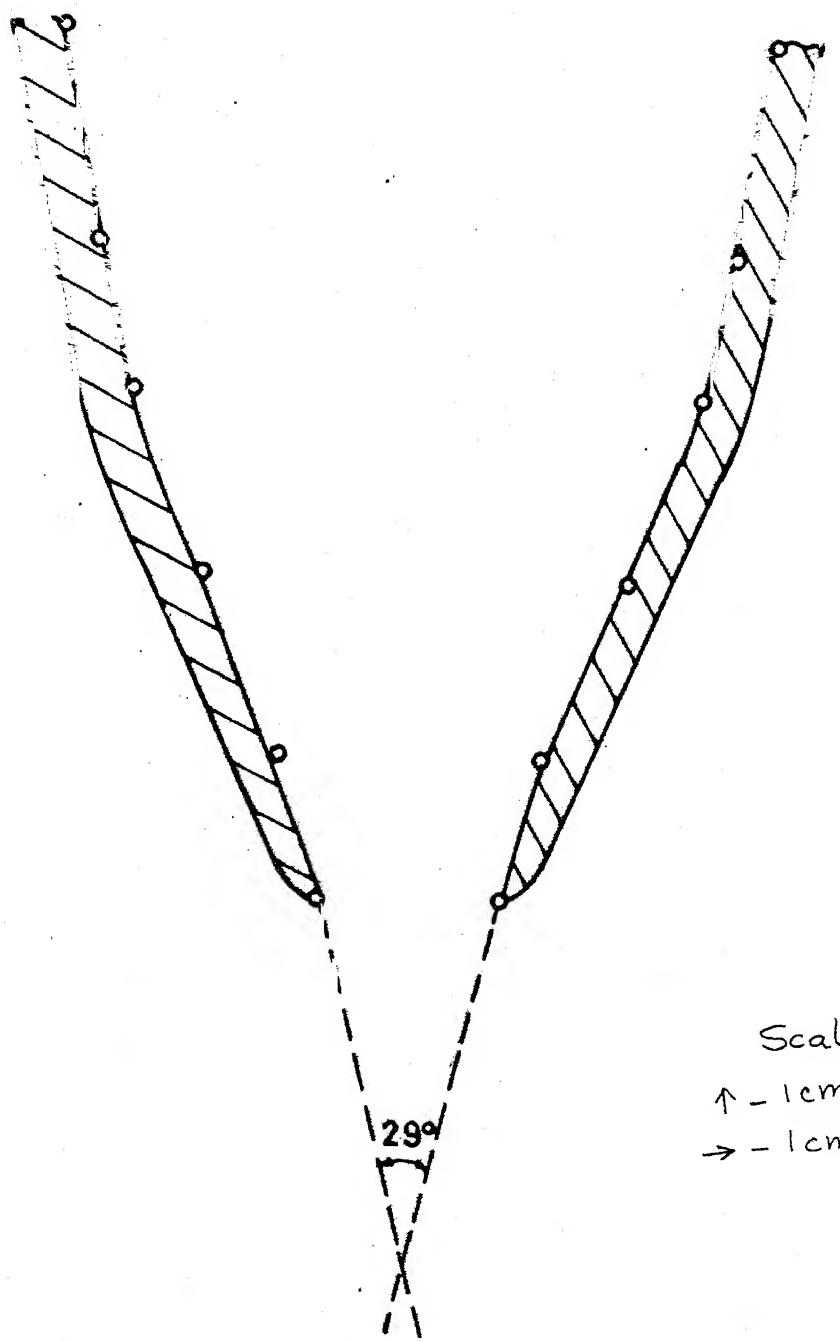

Fig. II.5(b) Sectional veiw of the nozzle profile of nozzle I ($\theta = 29^{o}$)

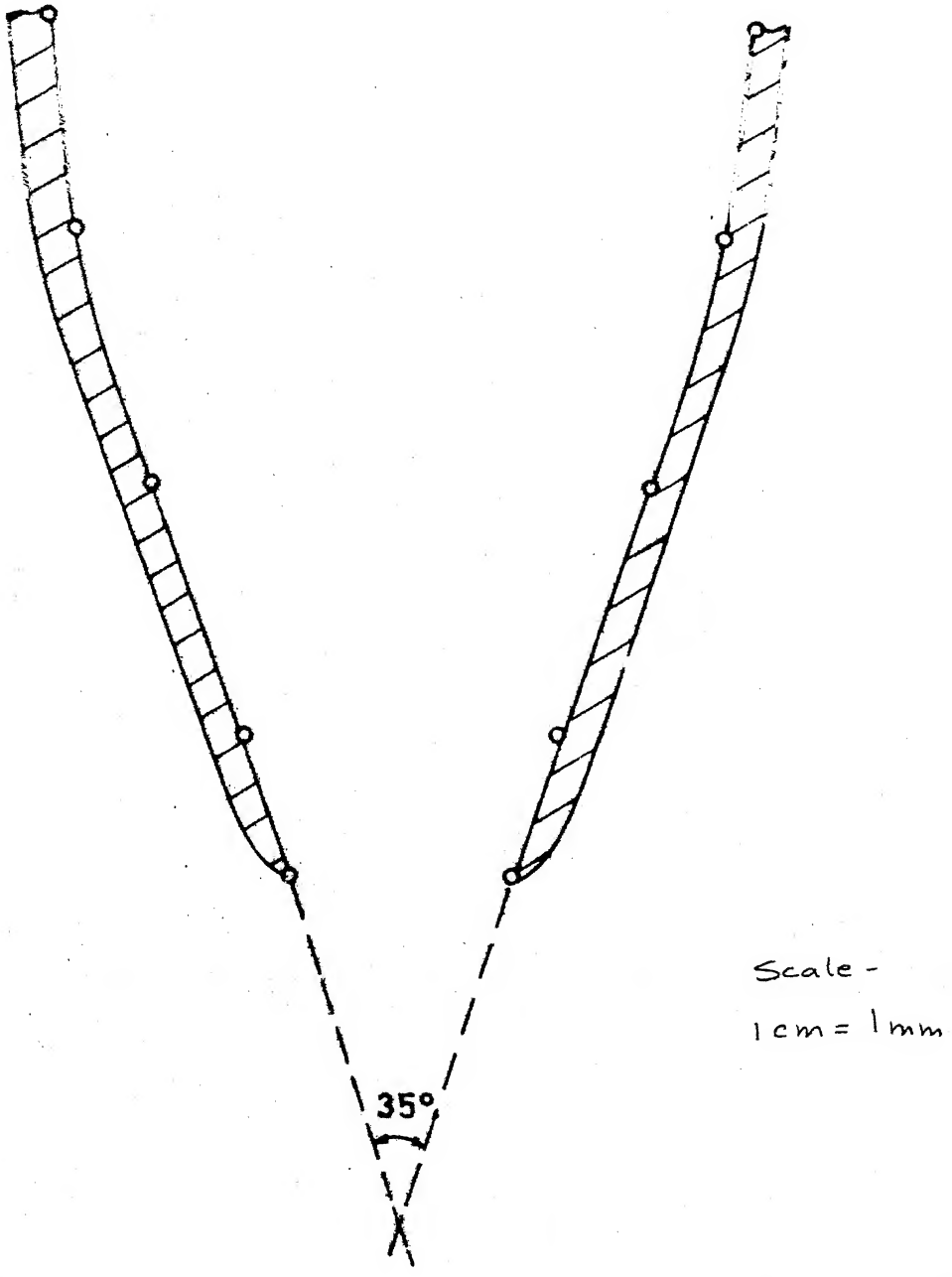

Fig. II.5(c) Sectional veiw of the nozzle profile of nozzle II ($\theta = 35^{o}$)

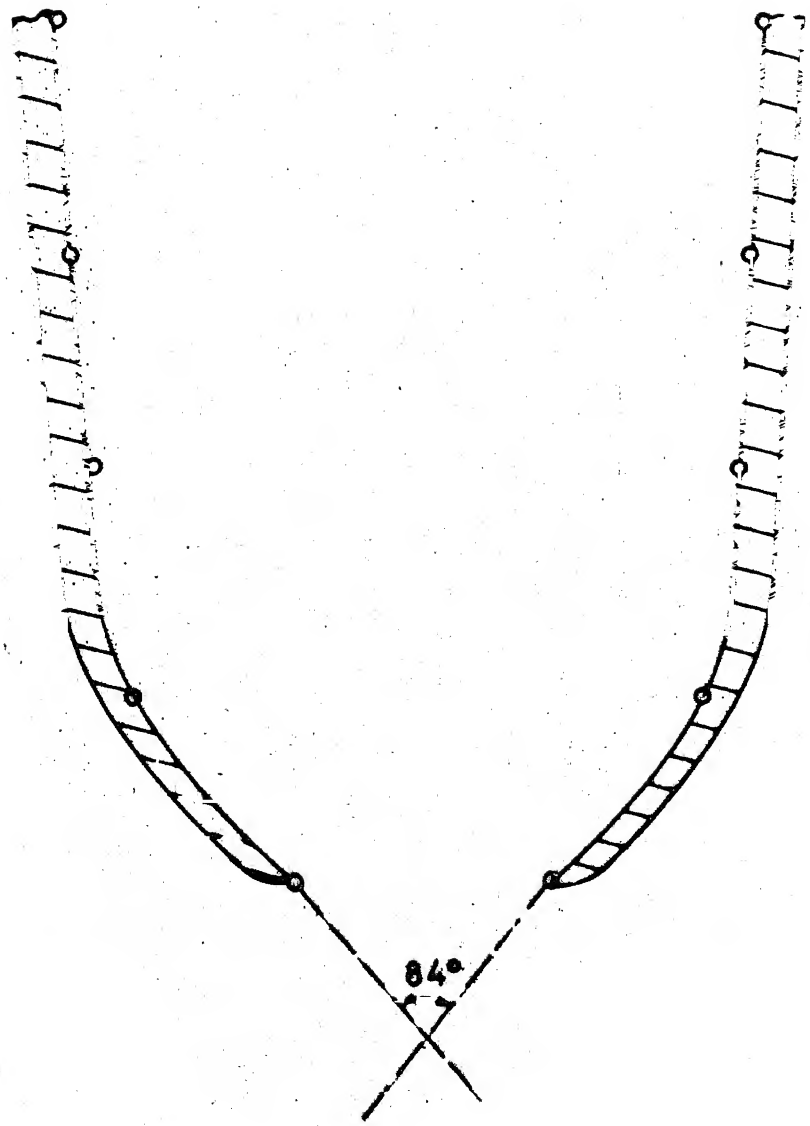

Scale-
1 cm = 1 mm.

Fig. II.5(d) Sectional veiw of the nozzle profile of nozzle III ($\theta = 84^{o}$)

II.4.2 MATERIAL

To study the effect of process parameters on the ribbon dimensions, commercial alumúnium was used. Alumunium rod of 8.5 mm diameter was cut into approx.10 mm long peices, were premelted to yield pellets which were then used for making wide ribbons.

II.4.3 WIDE RIBBON CASTING SET-UP

Melt spinning apparatus used (Figure II.6) has been described in detail by Chakachery[41]. It consists of a 23 cm diameter copper disc mounted on a 0.5 hp, DC motor whose speed can be varied from 0 - 3000 RPM. The alloy peiceswere placed in the nozzles and were heated by an induction coil powered by a 3 KW, 450 KHz rf generator. The diameter of the rf load coil was 16 mm at the upper end and gradually tapered down to 11 mm diameter at the lower end, consisting of total 6 turns. The total hieght of the coil was 19 mm. The slit orifice silica nozzles used for making wide ribbons were prepared as discussed in Section II.4.1. Snub nosed closed end tubes were used as crucibles for premelting the alloys. The premelting and the spinning operations were both done after evacuating and flushing the system thrice in succession with purified IOLAR II argon gas and a very feeble gas pressure was maintained during the operations. The full gas pressure was applied when the alloy had just melted completely (judged by visual inspection)

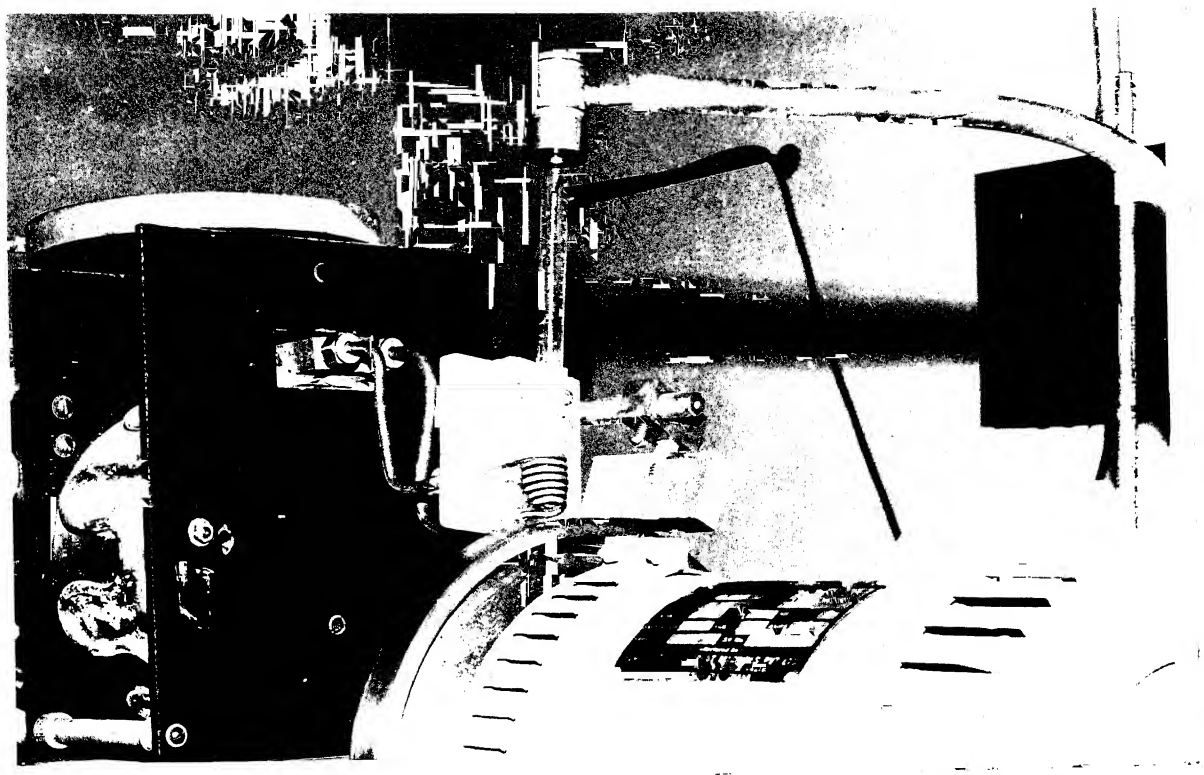

Fig. II.6 Photograph of the Chill Block Melt Spinning apparatus

for melt ejection. An air stopper, to reduce the melt puddle perturbation on the substrate was fixed just behind the nozzle, close to the copper wheel. It was made from a porspex peice and the lower end was lined with velvet cloth. The nozzle was held so that it's tip was 1 mm above the substrate. This distance could not be reduced furthur due to the geometry of the apparatus. After each run, the nozzle was cleaned and the same nozzle was repeatedly used for a series of experiments. During runs, all other parameters such as the distance between the induction coil and the substrate, axis of the nozzle with respect to the vertical direction etc. were kept constant.

II.5 RESULTS AND DISCUSSION

The variation of the ribbon thickness with the variation of ejection pressure ($\sqrt{P}$) is presented in Figure II.7. The thickness remains almost constant with the increase in pressure. This is in accordance to the experimental results obtained by Huang. It was observed by Huang[34] (Figure II.2) that the ribbon thickness, t is proportional to the square root of pressure, $\sqrt{P}$, at pressures lower than 2×10^4 Pa and then it saturates to a constant value, $t_{max.}$ when pressure is furthur raised. He derived that

$$t = \left[\frac{2\beta}{\rho V_s^2} \cdot \frac{w^3}{4\beta f h + w + c\beta w} \cdot P \right]^{1/2} \quad \ldots\ldots$$

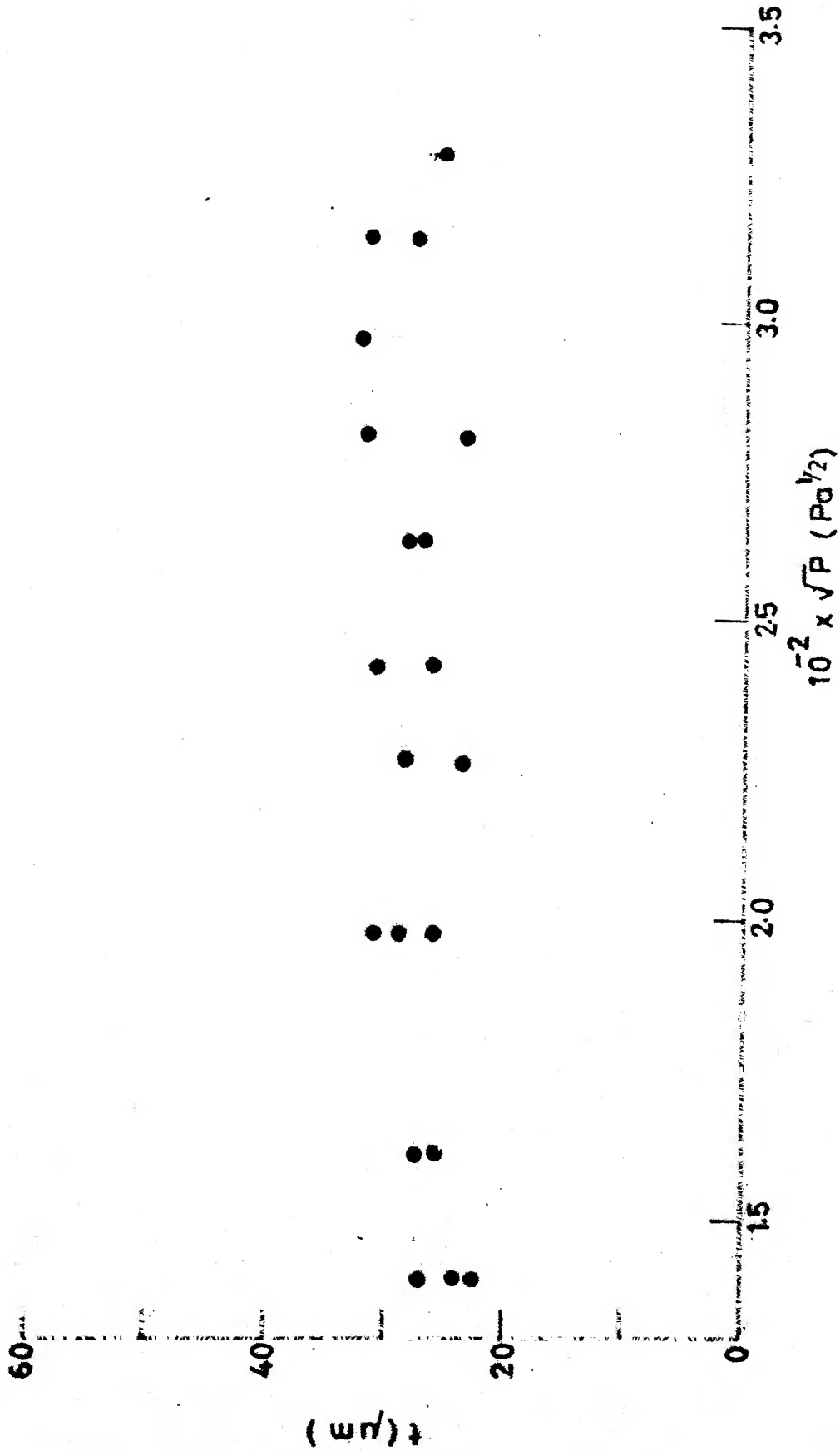

Fig. II.7 Ribbon thickness vs. square-root of ejection pressure

where w is the nozzle slot breadth, ρ is the liquid metal density, h is the hieght of the slot from the substrate and β, f and e are geometric coifficients. His experimental results on pressure dependence agreed with the above relation at low pressure regimes (below 2×10^4 Pa) but not at high values of pressures. The precise reason for this behaviour could not be given but was thought to be perhaps due to the forced flow of the melt in the wheel and nozzle gap at high applied pressures. The dependence of the thickness on the other parameters in the equation was not observed to be as expected from the equation above. In our case the pressures used by us were all higher than 2×10^4 Pa and the observed results agree with the results reported by Huang[34] and not as obtained by Liebermann and Graham[35]. Also the wheel speed, Vs did not seem to have it's effect on the ~~thickness~~ width of the cast ribbon during our investigations as shown in Figure II.8.

The plot of the variation of the ribbon width, w with the variation in ejection pressure is given in Figure II.9. The ribbon width is found to be proportional to the square root of ejection pressure, $\sqrt{P}$. According to the Bernouilli's equation[34],

$$\frac{P}{\rho} = \frac{e}{2} V_o^2 + 2f\left(\frac{h}{w}\right)V_o^2 + \frac{1}{2\beta} V_o^2$$

(where V_o is the velocity of the melt flowing out of the nozzle slot)

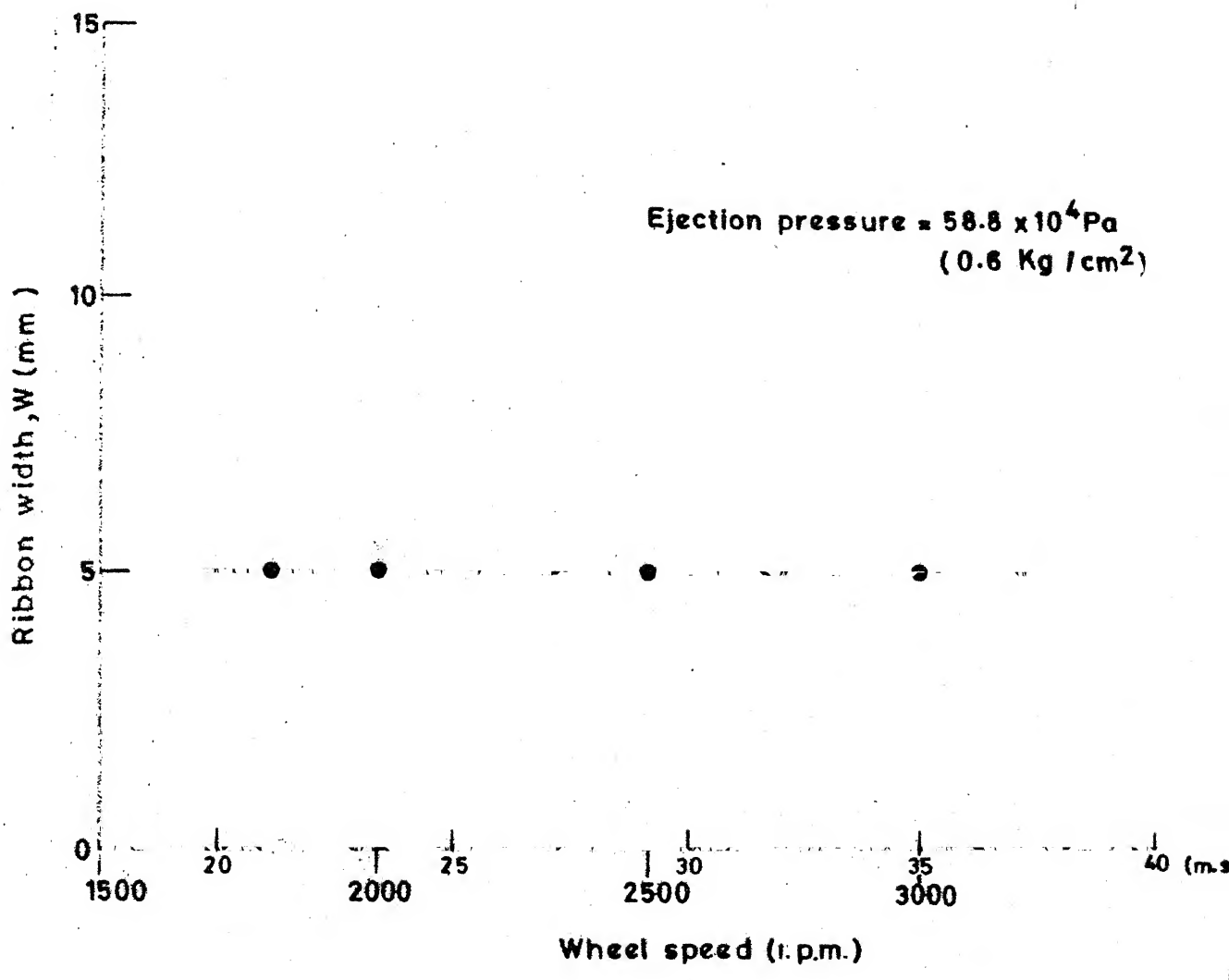

Fig. II.8 Ribbon width vs. wheel speed

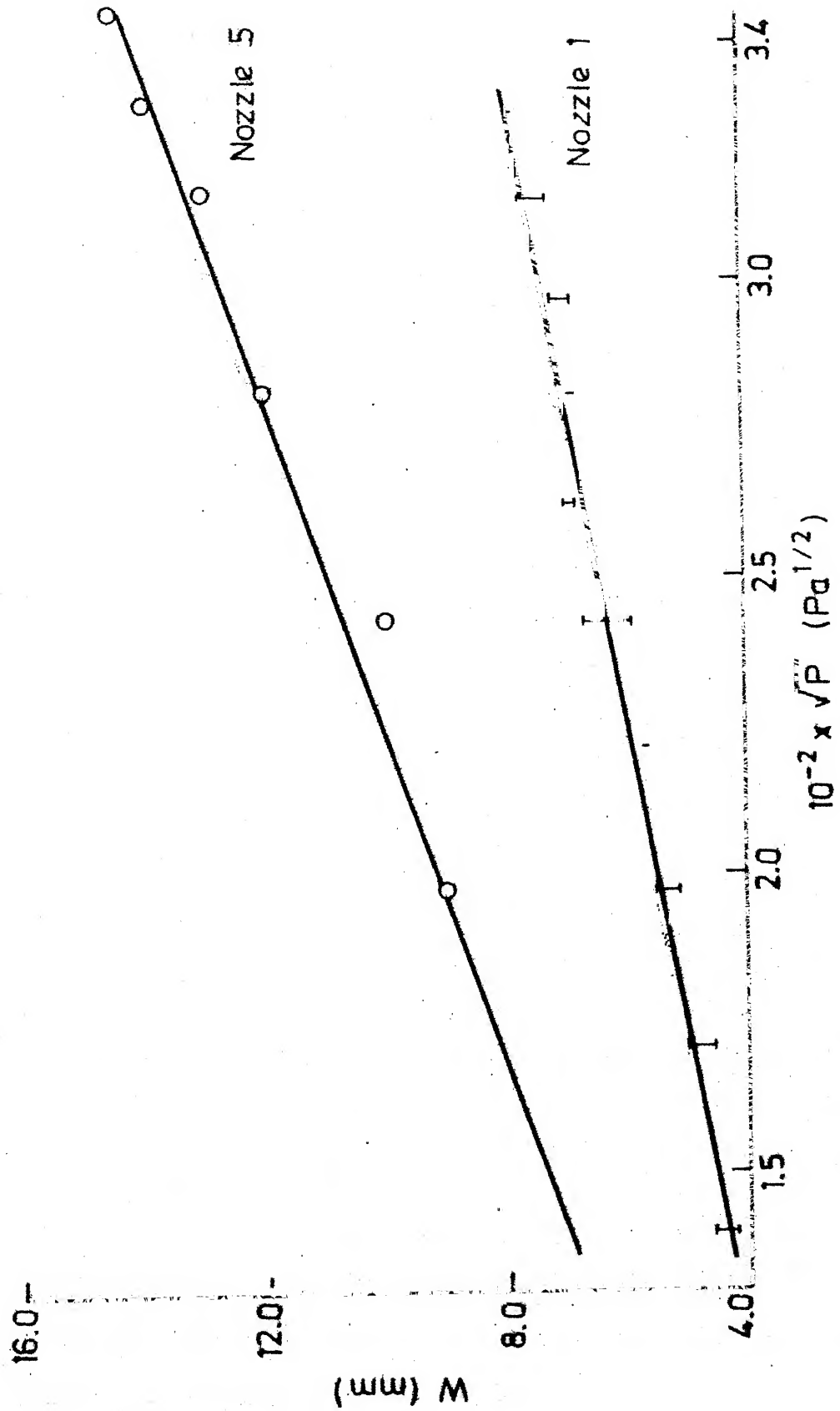

Fig. II.9 Ribbon width vs. square-root of ejection pressure

Square root of the ejection pressure is proportional to the melt flow velocity from the slot, V_o, which itself is proportional to the melt flow rate Q. Thus the square root of ejection pressure is proportional to the melt flow rate and as the melt flow rate governs the ribbon width, w,

$$w \propto \sqrt{P}$$

and our experimental results are found to agree with the above proportionality which we have derived.

The wetting pattern of the wheel side surface of the two ribbons cast under different ejection pressures are shown in Figure II.10 and Figure II.11 using the same nozzle and keeping other parameters unchanged. At low pressures, we observe that the air pockets are small irregular shaped and are distributed uniformly while at high pressure, larger air pockets are obtained. There was also found to be a variation in the wheel side surface of the ribbon from the centre towards the edges as shown in Figure II.12 and Figure II.13. This may arise due to a variation in the effective pressure along the width of the jet at the time of contact with the substrate.

The ribbon width, w has been found to be proportional to the nozzle angle, θ for various nozzles I,II and III having different slot dimensions (Figure II.5(b) to Figure II.5(d)) as shown in Figure II.14. Inspite of the difference in the slot dimensions, the ribbon width increases as we increase the nozzle angle, probably due to more melt spreading on the substrate.

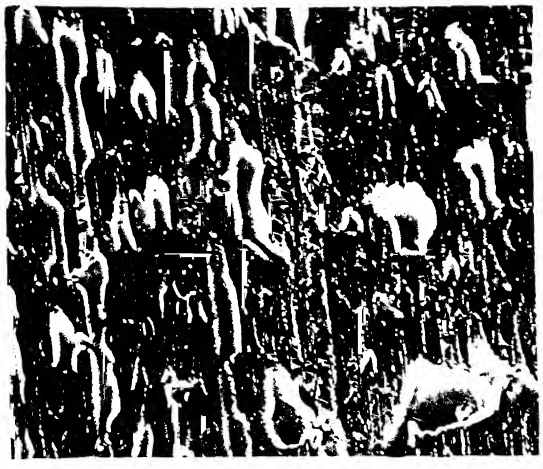

Fig. II.10 SEM photograph of the wetting pattern on the wheel side surface of a ribbon cast at $P = 19.6 \times 10^4$ Pa (250×)

Fig. II.11 SEM photograph of the wetting pattern on the wheel side surface of a ribbon cast at $P = 58.8 \times 10^4$ Pa (250×)

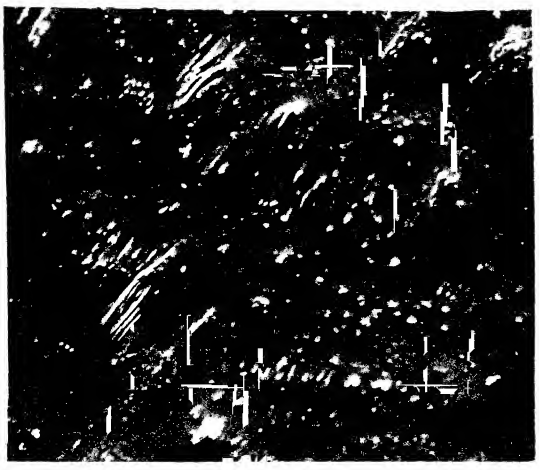

Fig. II.12 SEM photograph of the wheel side surface of the central region of a ribbon cast at $P = 39.2 \times 10^4$ Pa (100X)

Fig. II.13 SEM photograph of the wheel side surface of the edge region of a ribbon cast at $P = 39.2 \times 10^4$ Pa (100X)

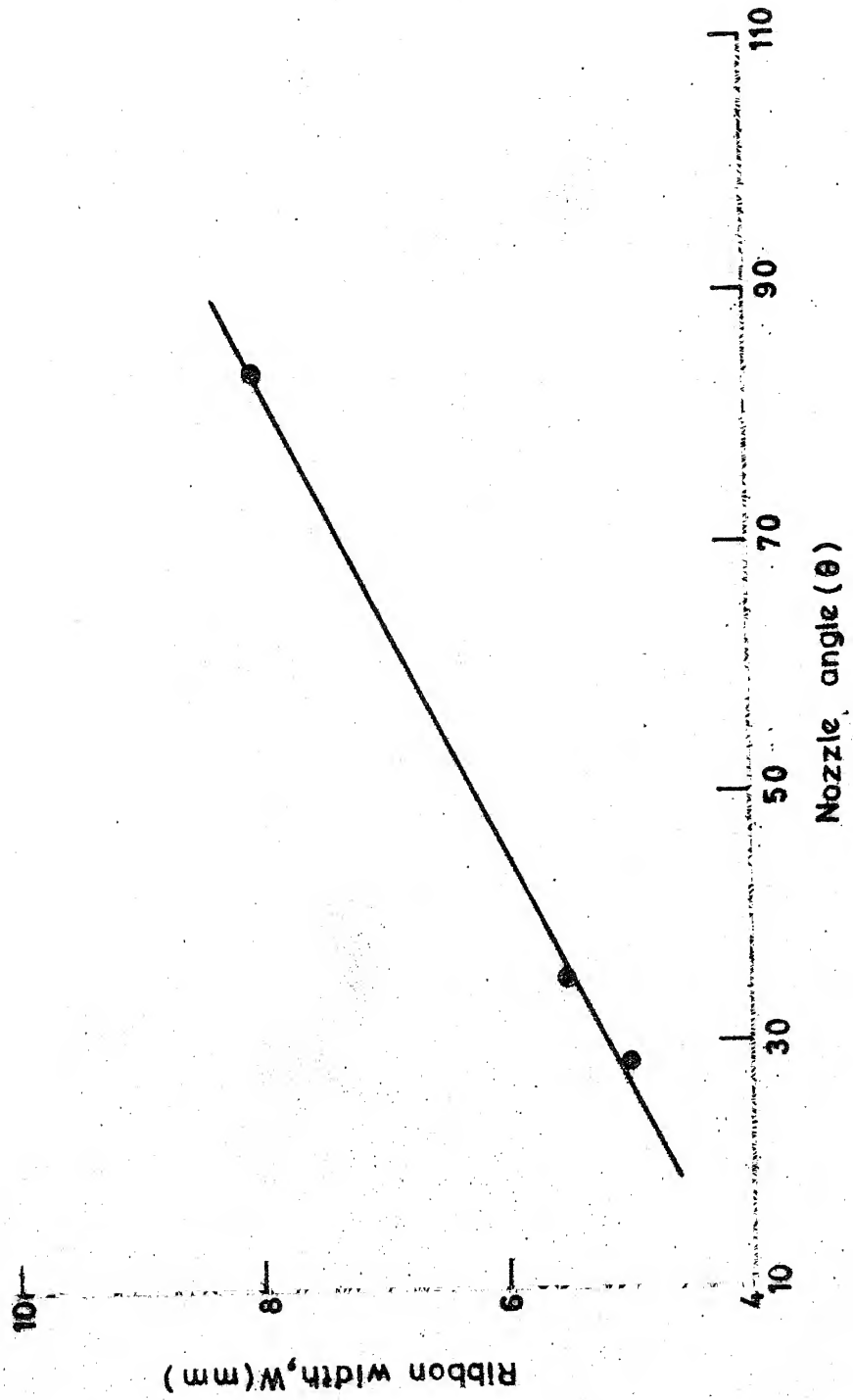

Fig. II.14 Ribbon width vs. nozzle angle

CHAPTER III

BRAZING OF 304 STAINLESS STEEL WITH Ni-BASE METALLIC GLASS FOILS

III.1 INTRODUCTION

The high temperature brazing process in the fabrication of structures utilizing metals has been the subject of continuing investigation[42-44]. Many alloys have been investigated for their capibality as brazing fillers to braze stainless steel[45-47]. The choice of the most suitable brazing alloy is usually a hit and trial process worked along a direction guided by published information. This is because there are a number of factors involved in the making and working of joints, which influence the results obtained. A number of applications pose their own specific requirements and specialized brazing alloys have to be developed for these uses. There are several considerations to be taken care of when choosing the correct filler for a perticular joining application as described in Chapter I. The nickel based series of fillers for stainless steel brazing covering a wide range of compositions have been developed for brazing stainless steel and have been listed in Table I.

Generally brazing is considered unsuitable as a joining process for joining stainless steel equipments/parts exposed to ammonia atmospheres due to agression[15], but as nickel based alloy with iron was found to be usable with boron

and silicon as melting point depressors. We chose a nickel based standard brazing alloy BNi-4 (which contains iron, boron and silicon) and also obtained two variations of it, by varing the iron content and studied the brazing process by using amorphous brazing foils of these alloys to braze stainless steel specimens and tried to evaluate the properties of the thus obtained brazed joints.

III.2 EXPERIMENTAL

III.2.1 TEST SPECIMENS

Austenitic steel of 18/8 type[(18 pct. Cr, 8 pct.Ni or (304 stainless steel)]was selected as the base metal. Stainless steel rods of 6 mm diameter were purchased from the local market and test specimens were machined as shown in Figure III.1(a). Two of these specimens were used for brazing end to end, yielding a brazed specimen as shown in Figure III.1(b). Test specimens as shown in Figure III.1(b) were also machined to test them for their strength and ductility for comparision with those of the brazed specimens. The surfaces to be joined were machined to a fine finish instead of being ground as it embeds the abrasive particles inside the surface of the sample and makes adhesion between the braze and the substrate weak. The samples were then cleaned by degreasing in acetone and rinsing with alcohol.

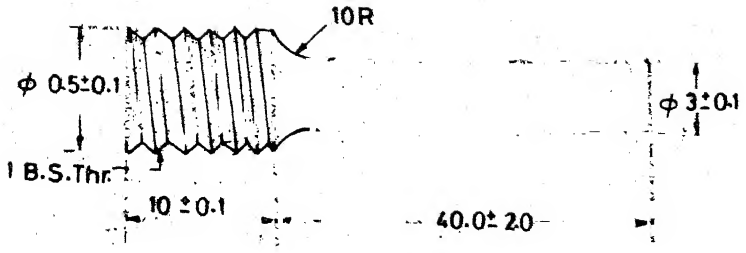

Fig.III.1(a) Brazing test specimen

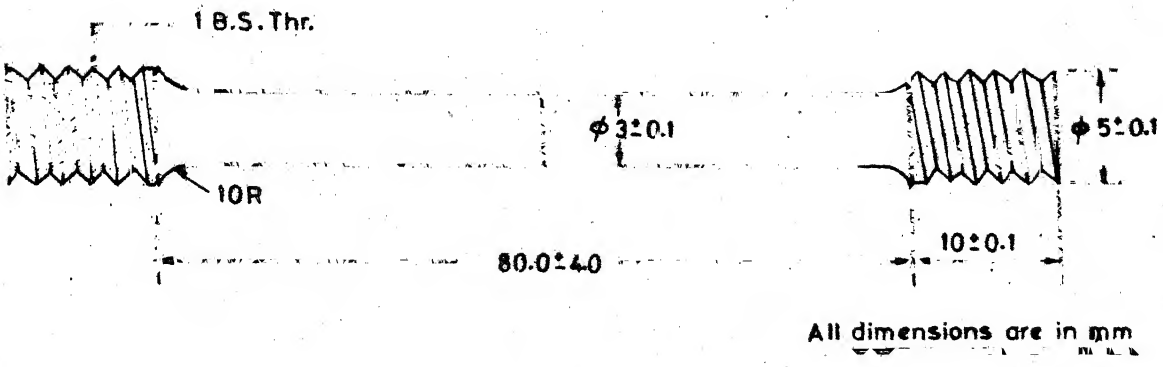

Fig.III.1(b) Brazed specimen

III.2.2 BRAZING FOILS

III.2.2(a) ALLOY PREPARATION

The alloys used for the preparation of brazing foils were prepared in an electric arc furnace which was locally assembled. A standard nickel based alloy BNi-4 (See Table I) having 1.5 wt.pct. iron and two variation of it, obtained by varing the iron percentage to 5 pct. and 10 pct. respectively, were prepared and subsequently foils of these three alloys were prepared and were used for brazing. Table III.1 shows the compositions of these alloys based on the amount of the various components used. The charge was placed in a copper crucible and an arc was stuck using a tungsten electrode after previously evacuating and flushing the system with argon for at least three successive cycles. The alloy preparation by striking the arc was done under argon atmosphere.

III.2.2(b) FOIL PREPARATION

As discussed in the last chapter, it was possible to prepare aluminium ribbons upto 8.5 mm wide. Attempts were therefore also made to prepare wide ribbons from the nickel based brazing alloys. However, although it was possible to obtain wide ribbons from these alloys, it was found that the ribbons had many holes. This could be the result of the break up of the melt puddle due to insufficient wetting of the substrate or the break up of the jet itself. The distance

between the nozzle tip and the substrate in planar flow casting is usually of the order of 0.3 mm. However, in our set up this distence could not be reduced below 1 mm due to excessive vibration of the wheel at the casting speeds. An experimental programme involving adjustment of parameters such as nozzle tip to substrate distance, substrate material, melt superheat etc. could not be carried out due to scarcity of time and also because although the foils had holes, they were otherwise quite suitable for the interded application i.e. brazing.

Brazing foils of the three alloys I,II and III (Table III.1) were prepared as described in Chapter II.

Table III.1

CHEMICAL COMPOSITIONS OF VARIOUS BRAZING FILLER ALLOYS

DESIGNATION		ELEMENTS (wt. pct.)			
Brazing alloy	AWS	Ni	Fe	B	Si
I	BNi-4	Bal.	1.5	3.5	4.0
II	-	Bal.	5.0	3.5	4.0
III	-	Bal.	10.0	3.5	4.0

The foils were found to be amorphous by X-Ray diffraction technique. The broad peak, charecterstic of the amorphous nature was obtained. Figure III.2 to Figure III.4 show the X-Ray

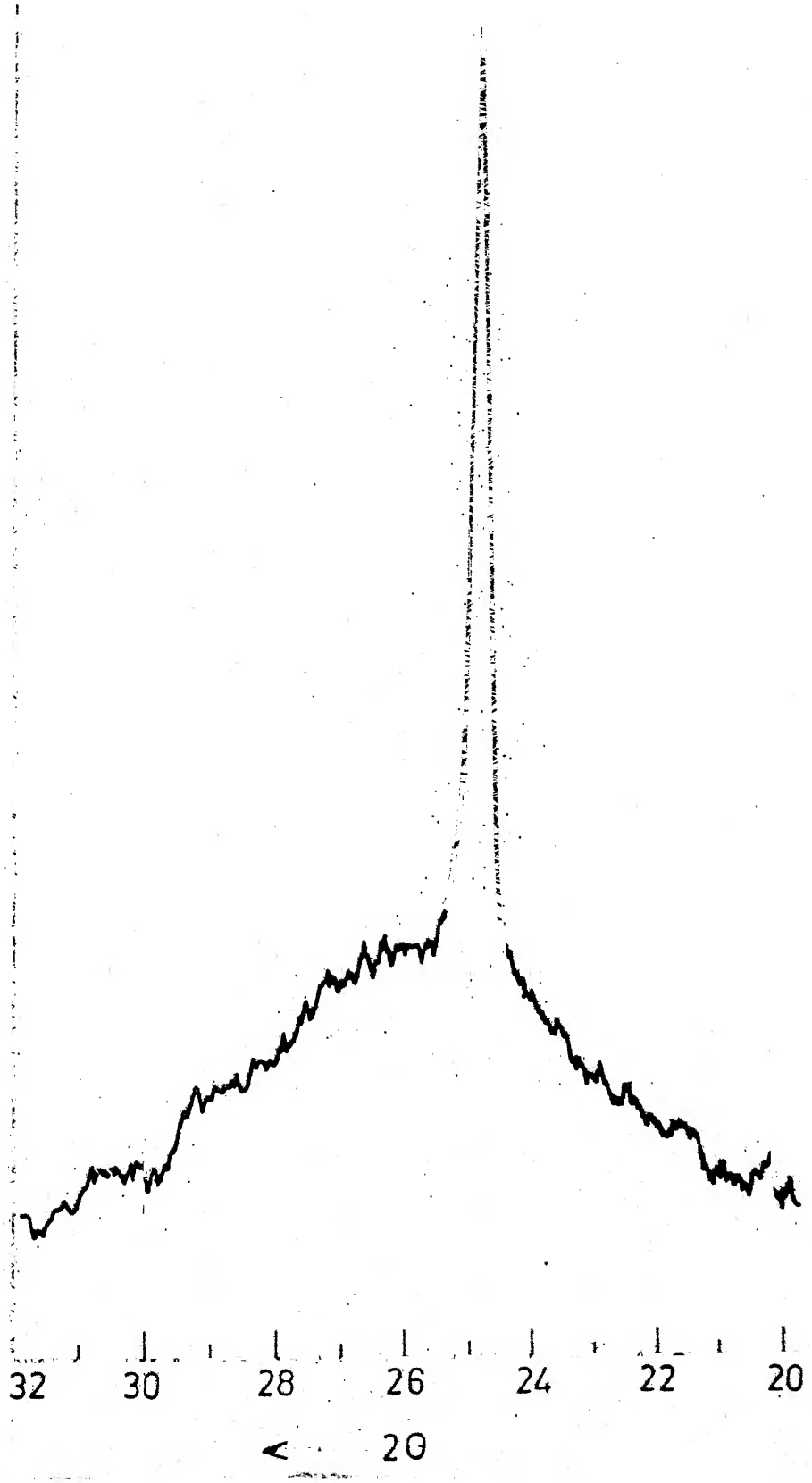

Fig.III.2 X-Ray diffraction pattern for amorphous nickel based brazing foil (sharp peak is from the Al holder)

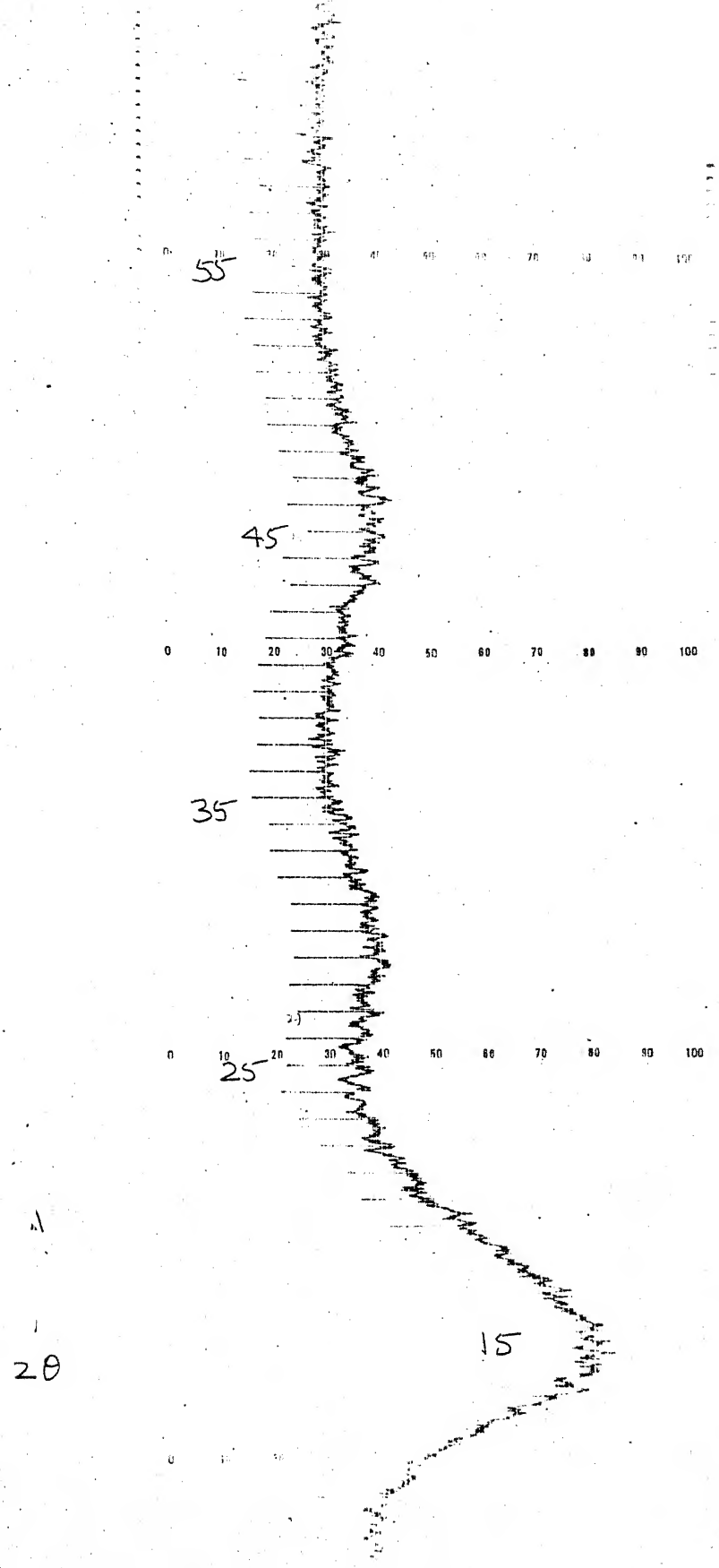

Fig.III.3 X-Ray diffraction pattern for amorphous nickel based brazing foil (using perspex holder)

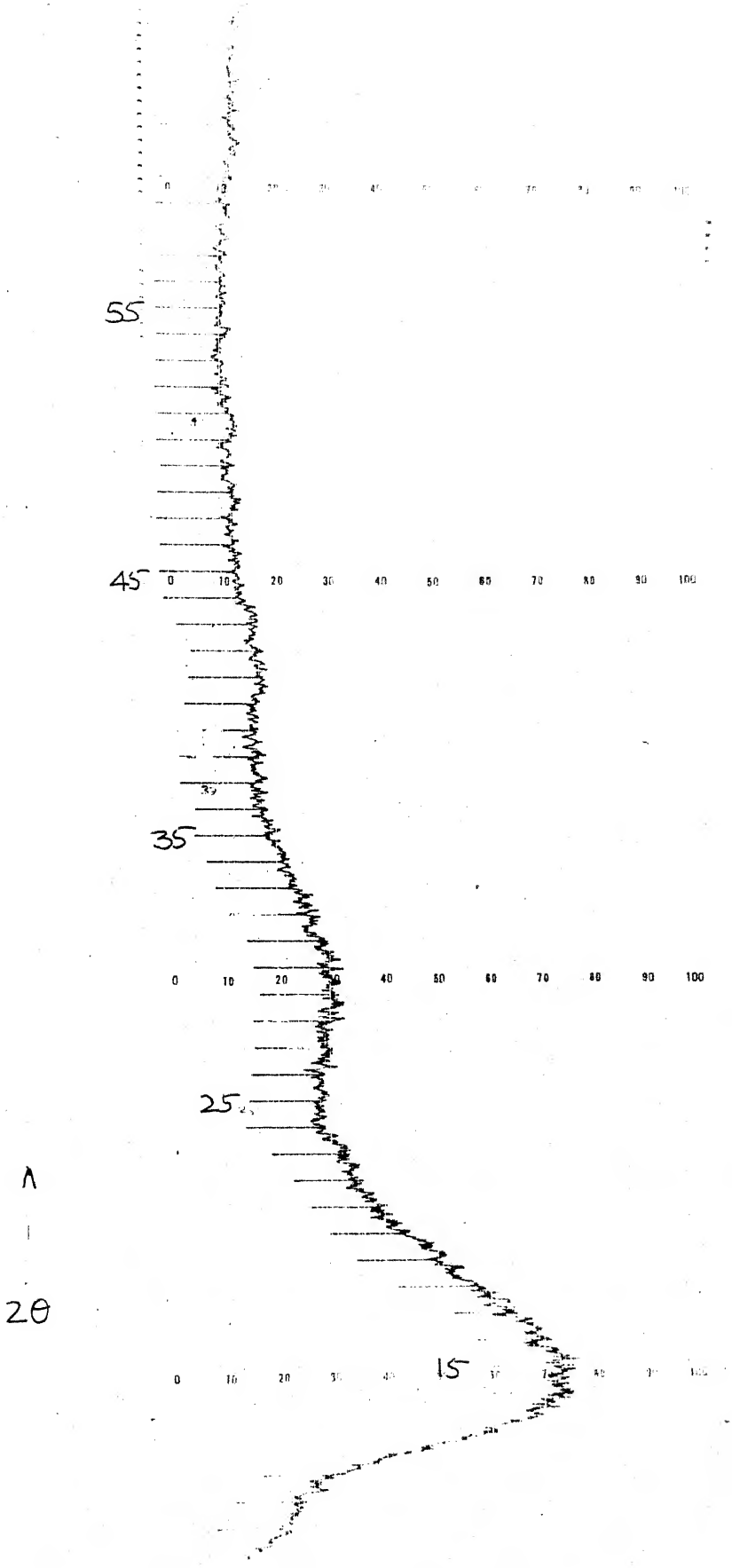

Fig.III.4 X-Ray diffraction pattern for perspex

diffraction patterns obtained. The fracture surface of the amorphous foils showing the typical vein structure was obtained as shown in Figure III.5. As a matter of interest, the fracture surface of a ribbon cast from alloy II at 18.25 m s^{-1}(1500 rpm) is also shown in Figure III.6. This ribbon was found to have crystalline peaks. The fracture surface is distinctly difference and does not have the vein pattern characteristic of the fully amorphous alloys. The foils used for brazing were 45 μm to 50 μm in thickness and 4 to 5 mm wide. They were used as discs of diameter slightly more than 3 mm (The ductile foils could be cut into disc shape and were preplaced in the joint prior to heating). Degreasing of the brazing discs was carried by immersion in acetone and thorough rinsing finally in methanol.

III.2.3 BRAZING SET-UP

The brazing operation was performed on a conventional vacuum coating unit. The ''Hind Hivac'' 12A4 vacuum coating unit was used. For performing the brazing of the stainless steel test speciments, modifications were made on the fixture usually used for carbon coating, using carbon rods. The specimens were screwed in two holders and the two holders were then themselves screwed in the sleeves meant to hold the carbon rods. The test specimens were then held face to face under compression by using a spring. The brazing foil was kept in between the two faces to finally obtain a butt brazed joint. The schematic

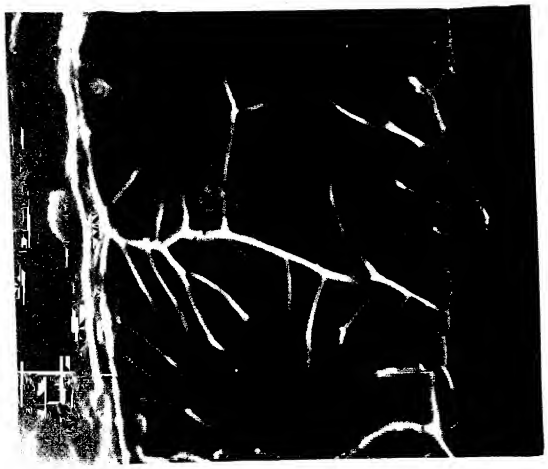

Fig.III.5 SEM photograph of the fracture surface of nickel based amorphous ribbon (Alloy II, $P = 58.8 \times 10^4$ Pa, $Vs = 30.09\ ms^{-1}$) (2000x)

Fig.III.6 SEM photograph of the fracture surface of nickel based ribbon, not fully amorphous. (Alloy II, $P = 58.8 \times 10^4$ Pa, $Vs = 18.25 ms^{-1}$) (2000X)

diagram of the set-up is shown in Figure III.7. The two test specimens were alligned to the best possible extent. Careful allignment of the two halves of the specimens is necessary because any misallignment would result in an apparent lowering of the observed strength of the joints during subsequent tensile testing as bending stresses would set up during the tensile test. Considerable effort was spent to ensure that the misallignment was as small as possible.

The brazing process was conducted under vacuum. The vacuum unit consisted of a mechanical pump and a diffusion pump. A vacuum level of 2×10^{-5} torr (267×10^{-5} Pa) was maintained during the operation in the bell jar in which the entire assembly was mounted. Resistance heating method was used to heat the joint area. Current was passed through the specimens from a low voltage high current power supply. The high resistance at the brazing foil-work peice contact caused heating to be maximum at the joint. The brazing temperatures by convention should be above the melting point of the filler alloy and below that of the base metal. Hence temperatures, 1180°C and above, but lower that the melting point of stainless steel were chosen for the various brazing operations. The temperatures were monitored by optical pyrometer. Also different brazing times were tried out at the various settings of temperature. The required temperatures could be reached within 30 Sec.

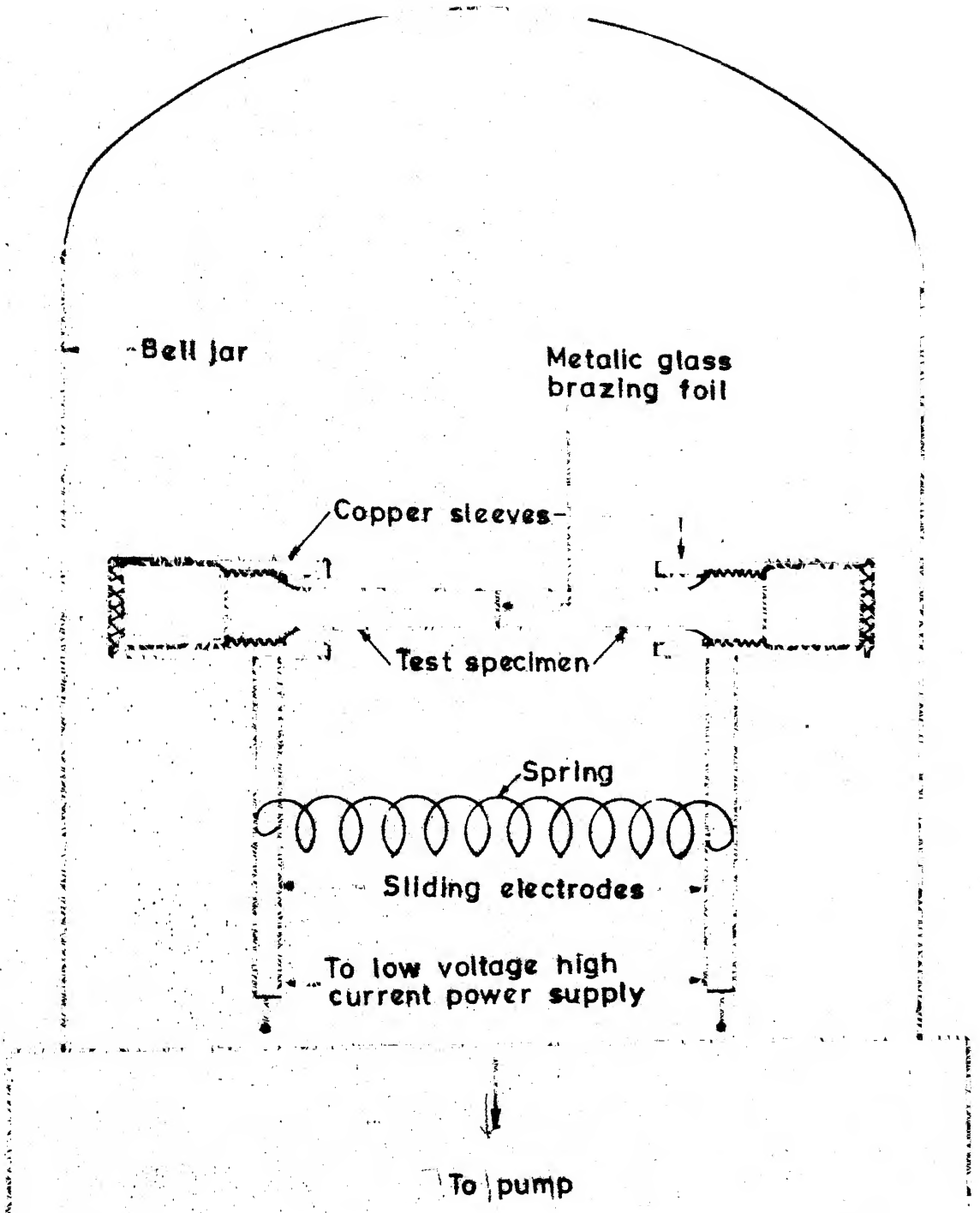

Fig.III.7 Schematic showing the set-up used for the brazing operation

A set of test specimens were also brazed using silver metal as a filler. The specimens were held in V-blocks and were torch brazed and were tested for strength and ductility by tensile testing them on Instron 1195 and the experimental results are presented later.

III.2.4 DETERMINATION OF BRAZING CONDITIONS

Several brazing temperature settings and brazing times were tried out to determine the best brazing conditions, i.e. resulting in brazements having maximum strength. The various temperatures used were 1180°C, 1220°C, 1260°C and 1350°C (as recorded by optical pyrometer) and brazing times of 90 Sec., 300 Sec. and 600 Sec. were tried out at each of these above mentioned temperatures. The maximum strength was obtained at 1260°C using a brazing time of 600 Sec. The details of the strength data are presented later.

III.2.5 CHARECTERIZATION OF THE BRAZED JOINTS

The following tests were selected to provide useful data in the consideration of the applicability of the brazing filler foils :

(a) Strength and Ductility

(b) Metallurgical structures

(c) Microhardness

III.2.5(a) STRENGTH AND DUCTILITY

The brazed test specimens were tensile tested on an Instron 1195 testing machine at a rate of 0.5 mm/Min. using a 1000 Kg. load cell. The load Vs elongation plots were recorded. The test were performed at room temperature. The tensile strengths were obtained by dividing the load by the origional cross-sectional area. The ductility or the percentage elongation was obtained by dividing the elongation by gauge length and multipling by 100. All the speciments failed in the brazed joint region.

III.2.5(b) METALLURGICAL STRUCTURES

To study the metallurgical structures prevailing at and around the brazed joint, the brazed test specimens were sectioned along the length to serve as metallographic specimens. For this a precision saw Microslice 2 (Metals Research Ltd., England) was used having a saw blade of 150 mm diameter with a diamond cutting edge. The sectioned peices were then mounted in bakelite and ground by using 2/0, 3/0 and 4/0 emery papers respectively and finally on a polishing wheel using 0.1 μm alumina powder. The ground and polished surfaces were then etched using a solution of ferric chloride and hydrochloric acid (5 gm. $FeCl_3$, 50 ml. HCl, 100 ml. distilled water). This was done for the joints brazed with alloys I,

II and III at 1260°C and 1350°C for 600 Sec. The micro structures were then studied using reflected light microscope.

III.2.5(c) MICROHARDNESS

The measurement of the hardness gradient requires the measurement of hardness over very small areas. Thus a Leitz Miniload 928003 microhardness tester was used to measure hardness variation across the brazed joint. The bakelite mounted ground and polished specimens (used to study the metallurgical structures) were used for the microhardness measurements also.

III.3 RESULTS AND DISCUSSIONS

III.3.1 STRENGTH AN DUCTILITY

The variation of the strength and ductility of the metallic glass ribbons of alloys I, II and III (1.5 mm to 2.0 mm wide and 40 μm to 50 μm thick) are presented in Table III.2. Measurements were done on an Instron 1195 testing machine using a 50 Kg. load cell at a cross head speed of 0.5 mm/Min. by mounting the ribbons on computer cards with the help of Quickfix.

We find that as the iron content in the brazing filler foil increases, the strength of the foil also increases. The ductility on the other hand falls with the increase in the iron content.

TABLE III.2

STRENGTH AND DUCTILITY

METALLIC GLASS RIBBONS

ALLOY	PERCENTAGE IRON	ULTIMATE TENSILE STRENGTH (MPa)	PERCENTAGE ELONGATION
I	1.5	1198.0	2.7
II	5.0	1851.8	1.6
III	10.0	2316.5	1.05

The strength and the ductility of the brazed specimens using the foils of the alloys I, II and III (brazed at 1260°C for 600 Sec.) are given in Figure III.8 and Figure III.9. The strength is found to increase with the increase of the iron content in the filler foil and ductility is found to be reduced as the iron content is raised. Thus there is a corelation between the strength of the ribbons and the strength of the joints. However the microstructures of the brazed joints differ appreciably as discussed later and the above correlation may be fortuitous. The results of the joint strengths for other brazing conditions are given in Table III.3. These conditions yield poorer results. Similar tensile tests with specimens brazed with silver filler gave a mean strength of 357.2 MPa and 10.7 percentage elongation. The strength of

TABLE III - 2 a

STRENGTH AND DUCTILITY OF JOINTS BRAZED AT 1260°c FOR 600 Sec.

ALLOY	Pct. IRON	ULTIMATE TENSILE STRENGTH (Mpa.)	Pct. ELONGATION
I	1.5	300	6.7
"	"	242	7.1
"	"	282	5.8
"	"	248	7.8
"	"	267	6.4
II	5.0	321	5.6
"	"	223	6.2
"	"	285	4.7
"	"	347	4.1
"	"	318	6.6
III	10.0	382	2.8
"	"	300	4.3
"	"	348	1.9
"	"	367	3.4
"	"	324	4.2

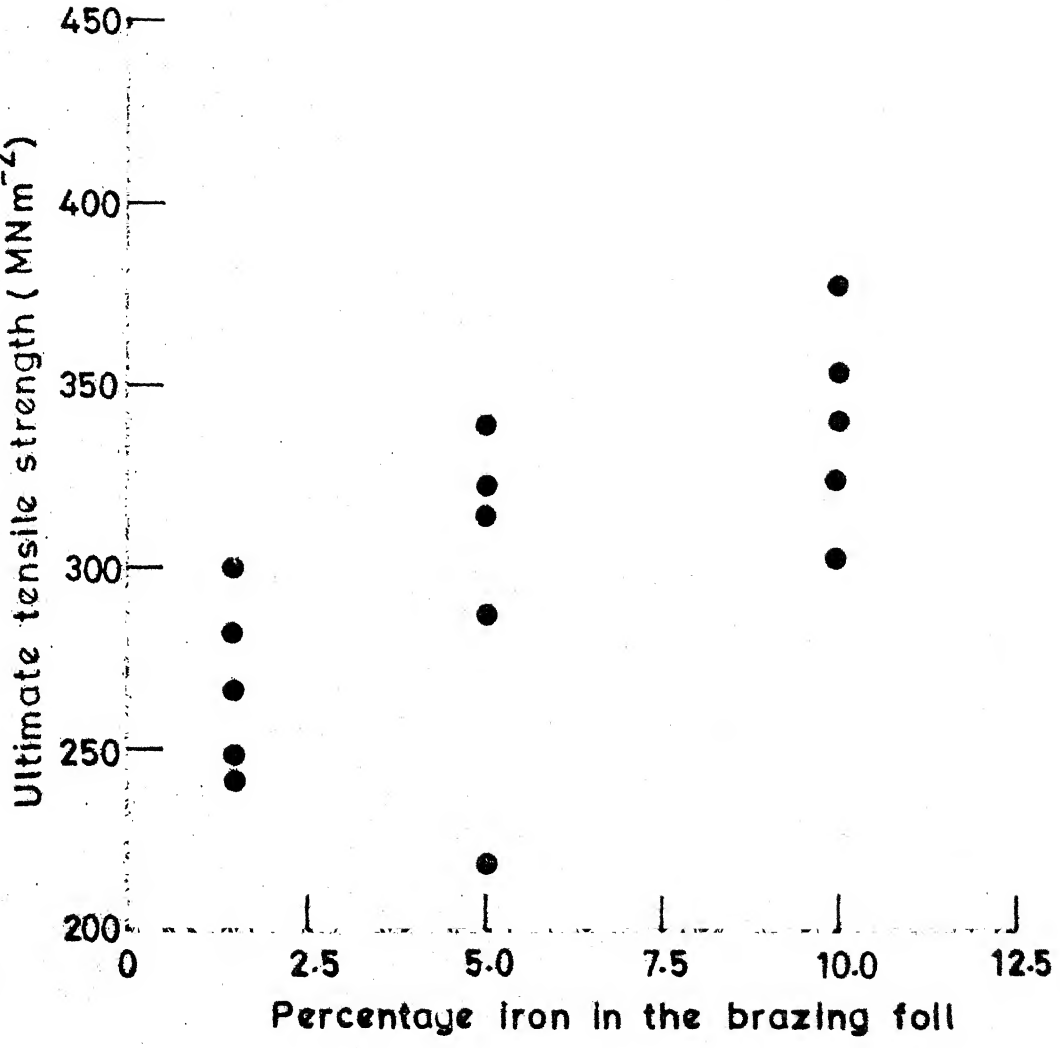

Fig.III.8 Variation in the strength of brazed joints with iron content in the brazing foil (1260°C, 600 sec)

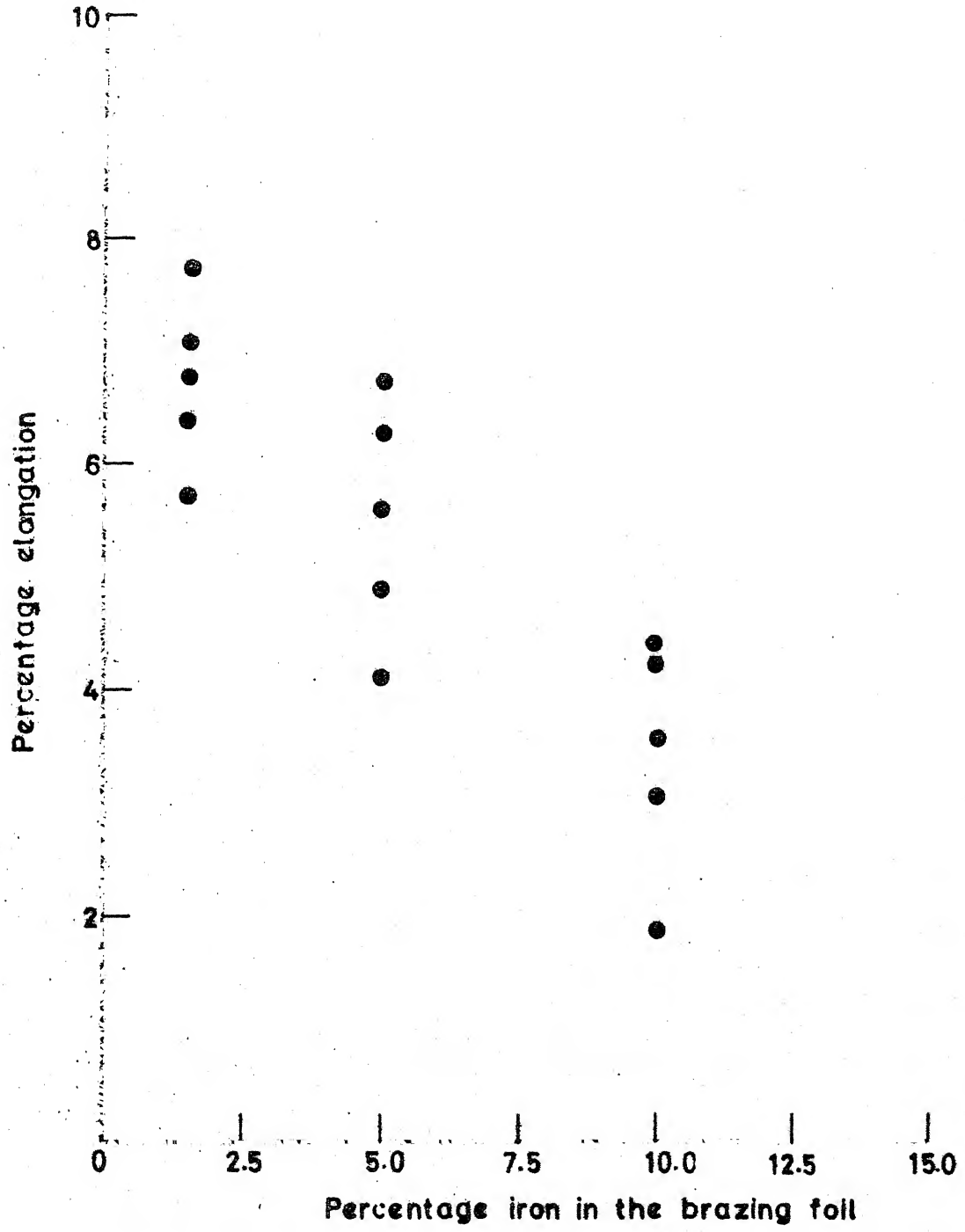

Fig.III.9 Variation in the ductility of brazed joints with iron content in the brazed joint (1260°C, 600 sec.)

TABLE III.3

STRENGTH AND DUCTILITY OF SPECIMENS

BRAZED UNDER VARIOUS BRAZING CONDITIONS

ALLOY	PERCENTAGE IRON	BRAZING TEMP. (°C)	BRAZING TIME (Sec.)	AVERAGE ULTIMATE TENSILE STRENGTH (MPa)	AVERAGE PERCENTAGE ELONGATION
I	1.5	1180	90	92.2	6.7
I	1.5	1180	300	106.0	5.3
I	1.5	1180	600	103.5	5.6
I	1.5	1220	90	65.4	7.6
I	1.5	1220	300	87.9	7.2
I	1.5	1220	600	79.7	8.3
I	1.5	1260	90	195.2	8.5
I	1.5	1260	300	208.4	7.6
I	1.5	1350	90	166.9	4.3
I	1.5	1350	300	172.2	4.8
I	1.5	1350	600	187.8	3.5
II	5.0	1180	90	120.0	6.6
II	5.0	1180	300	154.6	7.2
II	5.0	1180	600	138.4	5.9
II	5.0	1220	90	145.7	6.9
II	5.0	1220	300	137.6	5.7
II	5.0	1220	600	135.3	6.3

Table III.3 (Cont.)

ALLOY	PERCENTAGE IRON	BRAZING TEMP. (°C)	BRAZING TIME (Sec.)	AVERAGE ULTIMATE TENSILE STRENGTH (MPa)	AVERAGE PERCENTAGE ELONGATION
II	5.0	1260	90	227.4	4.8
II	5.0	1260	300	223.6	7.5
II	5.0	1350	90	197.0	3.8
II	5.0	1350	300	189.2	4.7
II	5.0	1350	600	182.4	5.2
III	10.0	1180	90	123.9	2.7
III	10.0	1180	300	109.8	3.9
III	10.0	1180	600	142.9	3.2
III	10.0	1220	90	154.7	4.3
III	10.0	1220	300	176.6	3.9
III	10.0	1220	600	179.2	3.8
III	10.0	1260	90	234.1	4.6
III	10.0	1260	300	267.3	4.2
III	10.0	1350	90	229.7	1.7
III	10.0	1350	300	245.0	2.9
III	10.0	1350	600	219.4	1.9

the stainless steel test specimens (Figure III.1(b)) was found to be 750 MPa and the ductility was found to be 28 pct.,which are both much higher than those obtained from the brazed specimens. The values of the strength of the joints brazed with metallic glass foils and silver filler are thus found to be comparable. The ductility of the silver brazed joints are found to be somewhat higher than the values obtained by using the amorphous foils as brazing fillers. The strength of the joints brazed with alloys I, II and III are also found to be comparable to the strength values of the joints brazed with nickel based amorphous foils reported in literature[17](given in Table III.4).

III.3.2 METALLURGICAL STRUCTURES

The details of the various structures observed in the case of the brazed sections using different alloys at 1260°C and 1350°C using 600 Sec. brazing times were studied. The thickness of the various structural zones as well as the total brazed region is least hear the centre of the specimen and increases as one goes towards the specimen surface. This is shown in a back scattered electron picture of a joint made with alloy III at 1260°C, brazed for 600 Sec. (Figure III.10).

MICROSTRUCTURAL ANALYSIS

ALLOY I (1.5 pct. Iron)

BRAZING TEMPERATURE - 1260°C

Figure III.11 shows the section through the joint along the length of the specimen brazed with brazing foil of

TABLE III.4

STRENGTH OF BRAZED JOINTS USING

VARIOUS FILLER METALS

IGNATION	FOIL COMPOSITION, wt.pct.							ULTIMATE TENSILE STRENGTH (MPa)	COMMENTS
	Cr	Si	B	Fe	C	Au	Ni		
Ni-1	13.0-15.0	4.0 - 5.0	2.75-3.50	4.0-5.0	0.06	-	Bal	457	Failed in base metal
-	12.0-14.0	4.0 - 5.0	2.5 - 3.2	3.5-5.0	0.03	-	Bal	490	Failed in base metal
Ni-2	6.0-8.0	4.0 - 5.0	2.75-3.50	2.5-3.5	0.06	-	Bal	432	Failed in joint
Ni-3	-	4.0 - 5.0	2.75-3.50	0.5	0.06	-	Bal	463	Failed in base metal
-	14.5-16.0	-	3.17-4.20	-	-	-	Bal	468	Failed in base metal
-	-	-	-	-	-	81.5-82.5	Bal	505	Failed in base metal

(Reference 17)

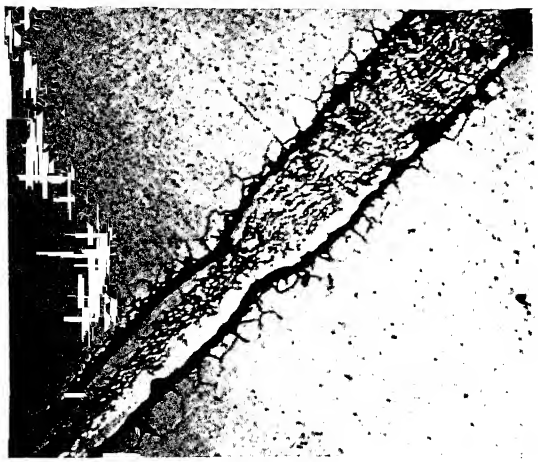

Fig. III.10 BSE photograph of a brazed joint, sectioned along the length (36×)

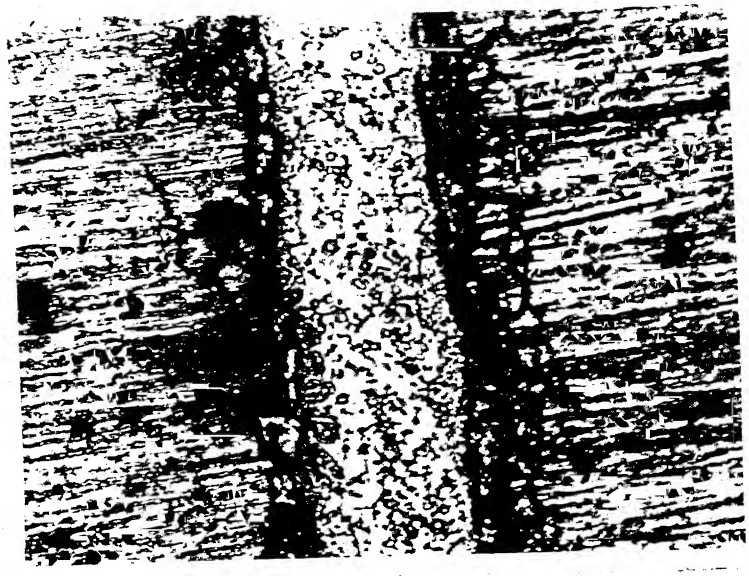

Fig. III.11 Micrograph of the brazed joint (1260°C, 600 Sec.), sectioned along the length, using brazing foil of alloy I (600X)

Fig. III.12 Micrograph of the brazed joint (1260°C, 600 Sec.), sectioned along the length, using brazing foil of alloy II (600X)

alloy I at 1260°C for 600 Sec. Four different regions are observable in the brazed section. The central region (I) consists of equiaxed or dendritic structure. Then it is followed by region(II) which consists of a mixture of fine bright and grey phases. Then the next region (III) comprises of thick dark grain boundaries and the last region consists of dark and bright needle like structure (IV) in the base metal. The region II solidifies faster due to conduction of heat through the sample, giving rise to a fine grained structure while the region I cools slowly resulting in larger equiaxed grains or dendritic structures. The extent of these various regions at the centre of the brazed sections and near the surface of the specimen are different and can be seen in Table III.5.

TABLE III.5

VARIOUS REGION. LENGTHS IN THE BRAZED SECTION

POSITION OF THE VEIWING SECTION	REGION III (mm)	REGION II (mm)	REGION I (mm)	TOTAL BRAZED REGION (mm)
Near Surface (End I)	0.035	0.015	0.02	0.115
	0.035	0.01		
Centre	0.025	0.01	0.015	0.09
	0.03	0.01		
Near Surface (End II)	0.03	0.01	0.03	0.11
	0.03	0.01		

ALLOY II (5.0 pct. Iron)

BRAZING TEMPERATURE - 1260°C

The regions I, II and III as observed in brazed sections with alloy I (1260°C, 600 Sec.) are also observed in sections brazed with alloy II (1260°C, 600 Sec.), but region IV is not observed as can be seen in Figure III.12. Table III.6 gives the details of the various zone lengths.

TABLE III.6

VARIOUS REGION LENGTHS IN THE BRAZED SECTION

POSITION OF THE VEIWING SECTION	REGION III (mm)	REGION II (mm)	REGION I (mm)	TOTAL BRAZED REGION (mm)
Near Surface (End I)	0.09	0.03	0.045	0.265
	0.09	0.01		
Centre	0.035	0.02	-	0.085
	0.03			
Near Surface (End II)	0.045	0.04	0.03	0.205
	0.06	0.03		

ALLOY III (10.0 pct. Iron)

BRAZING TEMPERATURE - 1260°C

All the four different regions observed in the case of alloy I (1260°C, 600 Sec.) were there in sections brazed with alloy III (1260°C, 600 Sec.) as shown in Figure III.13. The details of the different resion lengths are given in Table III.7.

TABLE III.7

VARIOUS REGION LENGTHS IN THE BRAZED SECTION

POSITION OF THE VEIWING SECTION	REGION III (mm)	REGION II (mm)	REGION I (mm)	TOTAL BRAZED REGION (mm)
New Surface (End I)	0.08	0.03	0.11	0.315
	0.055	0.04		
Centre	0.06	0.03	0.03	0.22
	0.065	0.035		
New Surface (End II)	0.04	0.03	0.04	0.175
	0.045	0.02		

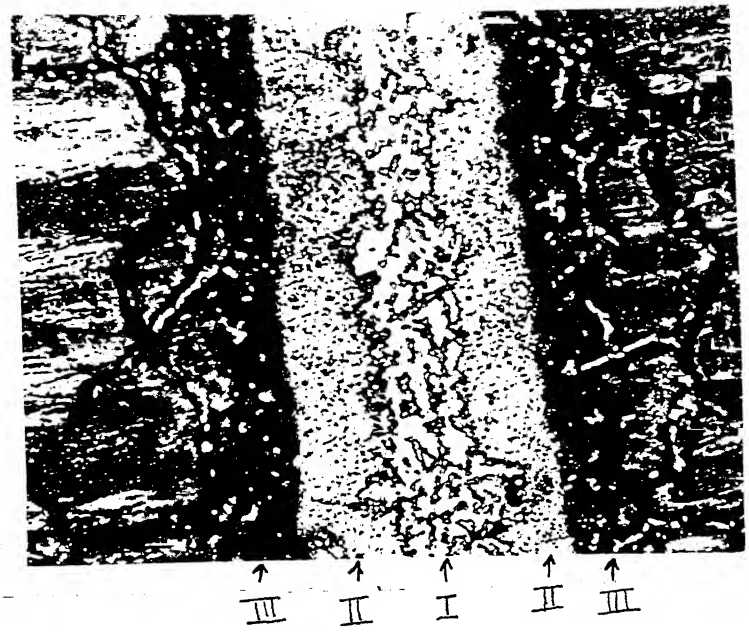

Fig. III.13 Micrograph of the brazed joint (1260°C, 600 Sec.), sectioned along the length, using brazing foil of alloy III (300x)

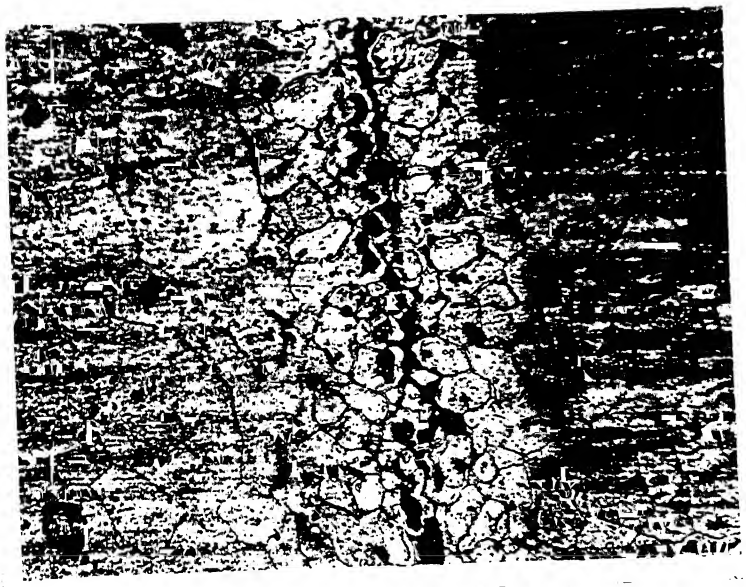

Fig. III.14 Micrograph of the brazed joint (1350°C, 600 Sec.), sectioned along the length, using brazing foil of alloy I (300x)

ALLOY I (1.5 pct. Iron)

BRAZING TEMPERATURE - 1350°C

The central region I is absent in this case which was previously observed for sections brazed with alloys I, II, III (1260°C, 600 Sec.). The brazed section using alloy I (1350°C, 600 Sec.) instead shows recrystallized grains of stainless steel. The braze metal seems to have mostly diffused into the base metal and only a thin central molten zone remains producing a thin dark molten zone in the centre of the brazed region as shown in Figure III.14. The widths of these regions are given in Table III.8

TABLE III.8

VARIOUS REGION LENGTHS IN THE BRAZED SECTION

POSITION OF THE VEIWING SECTION	RECRYSTALLIZED GRAIN REGION (mm)	DARK REGION (mm)	TOTAL BRAZED REGION (mm)
Near Surface (End I)	0.05 0.045	0.005	0.10
Centre	0.06 0.055	0.01	0.125
Near Surface (End II)	0.065 0.065	0.005	0.135

ALLOY II (5.0 pct. Iron)

BRAZING TEMPERATURE - 1350°C

The dark region at the centre and the recrystallized grains are both observable in the sections brazed with alloy II (1350°C, 600 Sec.) as shown in Figure III.15. The details of these zone lengths are given in Table III.9.

TABLE III.9

VARIOUS REGION LENGTHS IN THE BRAZED SECTION

POSITION OF THE VEIWING SECTION	RECRYSTALLIZED GRAIN REGION (mm)	DARK REGION (mm)	TOTAL BRAZED REGION (mm)
Near Surface (End I)	0.04 0.03	0.12	0.19
Centre	0.095 0.02	0.015	0.13
Near Surface (End II)	0.055 0.05	0.19	0.295

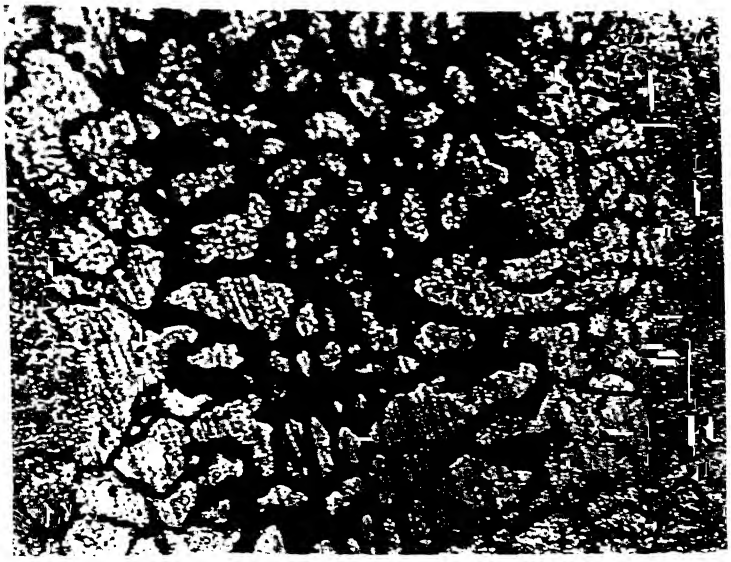

Fig. III.15 Micrograph of the brazed joint (1350°C, 600 Sec.), sectioned along the length, using brazing foil of alloy II (600x)

Fig. III.16 Micrograph of the brazed joint (1350°C, 600 Sec.), sectioned along the length, using brazing foil of alloy III (600x)

ALLOY III (10.0 pct. Iron)

BRAZING TEMPERATURE - 1350°C

Recrystallized grains and central dark regions as observed in brazed sections using alloys I and II (1350°C, 600 Sec.) are also observed in section brazed using alloy III (1350°C, 600 Sec.) as shown in Figure III.16. The lengths of these regions are given in Table III.10

TABLE III.10

VARIOUS REGION LENGTHS IN THE BRAZED SECTION

POSITION OF THE VEIWING SECTION	RECRYSTALLIZED GRAIN REGION (mm)	DARK REGION (mm)	TOTAL BRAZED REGION (mm)
Near Surface (End I)	0.055 0.08	0.135	0.27
Centre	-	0.005	0.005
Near Surface (End II)	0.06 0.06	0.25	0.37

The total brazed region is found to be maximum under both 1260°C and 1350°C brazing temperatures (600 Sec.), when the iron content in the brazing foil is maximum. This may be due to the increased agression in the base metal with the increase in iron content. This corresponds to the result reported in literature [48] of maximum agression in iron containing nickel based filler used brazements as compared to the other nickel based filler brazed sections.

III.3.3 MICROHARDNESS

The microhardness profiles of the joints brazed with alloys I,II and III at 1260°C (600 Sec.) are given in Figure III.17 to Figure III.19. The maximum value of hardness is observed in the central region (I). Then it goes through a minima and then again rises followed by a dip and a furthur rise to value of the base metal.

The microhardness profiles of the joints brazed with the same alloys at 1350°C (600 Sec.) are shown in Figure III.20 to Figure III.22. The hardness values are low in the central dark region, rises to a sharp maxima in the recrystallized region and then after going through a minima (not for Alloy III) rises to the value of the base metal.

The microhardness profile has been found to more or less follow the boron concentration profile in the brazed sections using metallic glass foils[13] by earlier workers. The difference in composition and the phases in the various regions result in a variation in the hardness values. However as the X-Ray chemical analysis facility was not available with the scanning electron microscope, such a correlation could not be made in our case.

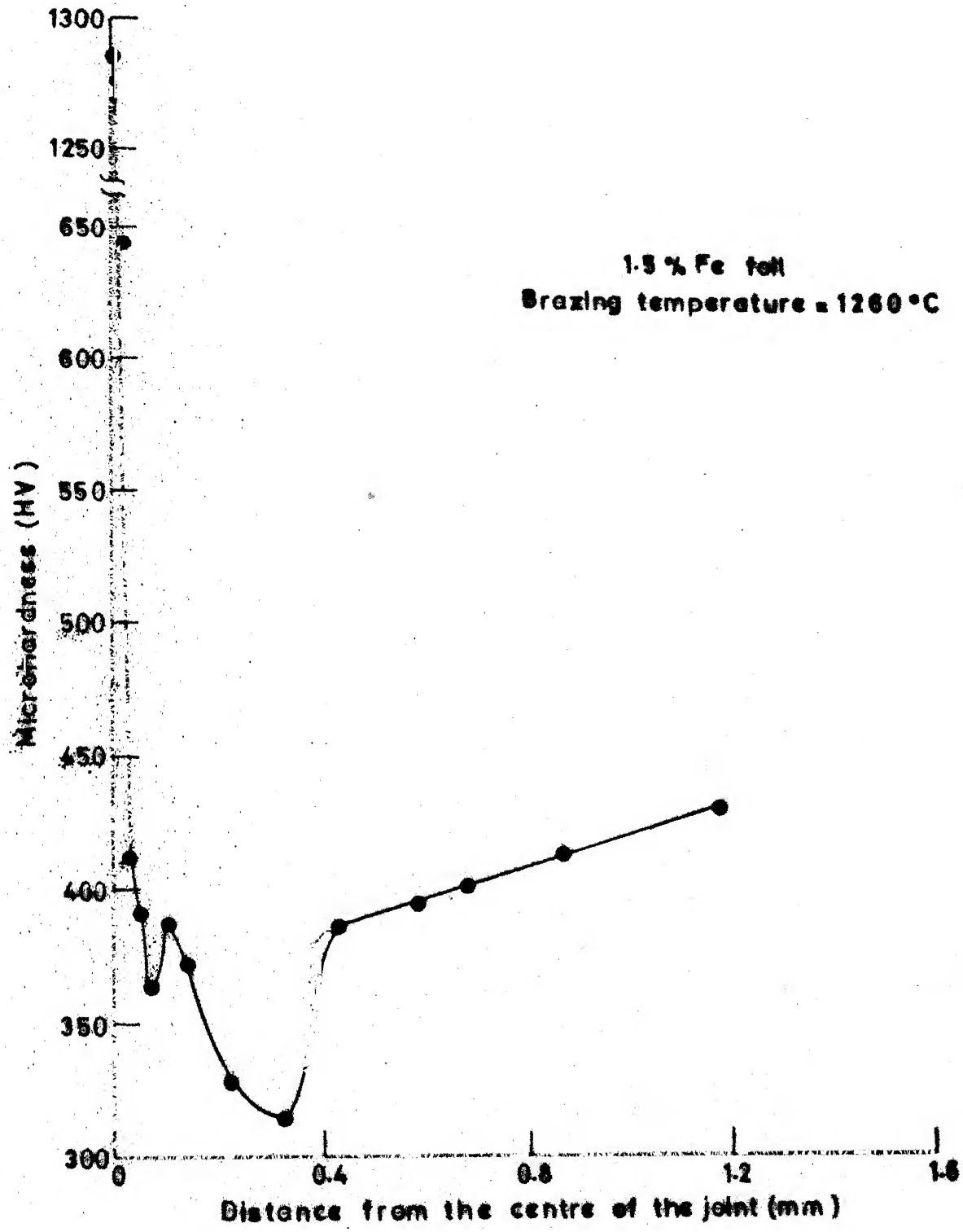

Fig. III.17 Microhardness profile across the brazed section (Alloy I, 1260°C, 600 Sec.)

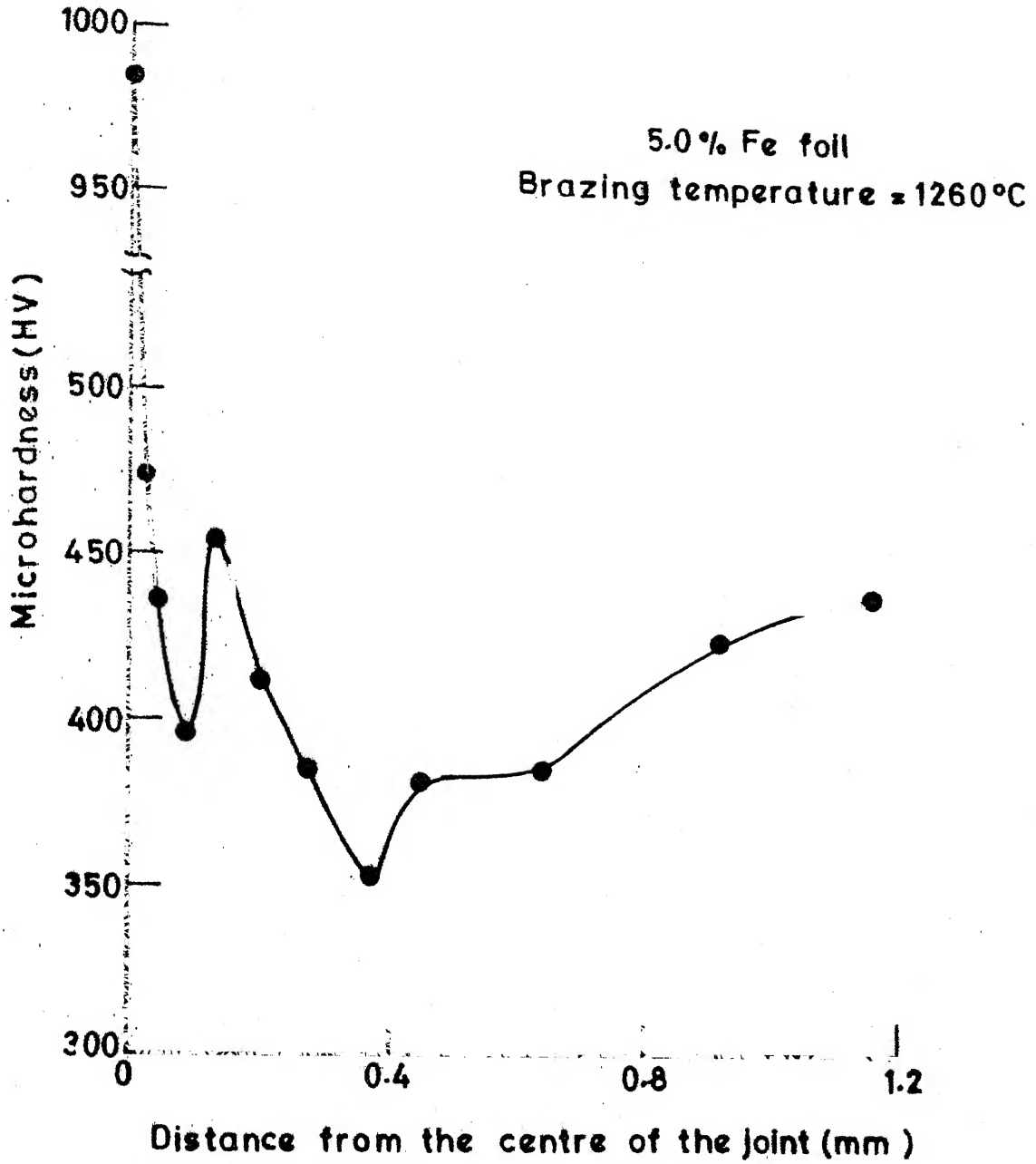

Fig. III.18 Microhardness profile across the brazed section (Alloy II, 1260°C, 600 Sec.)

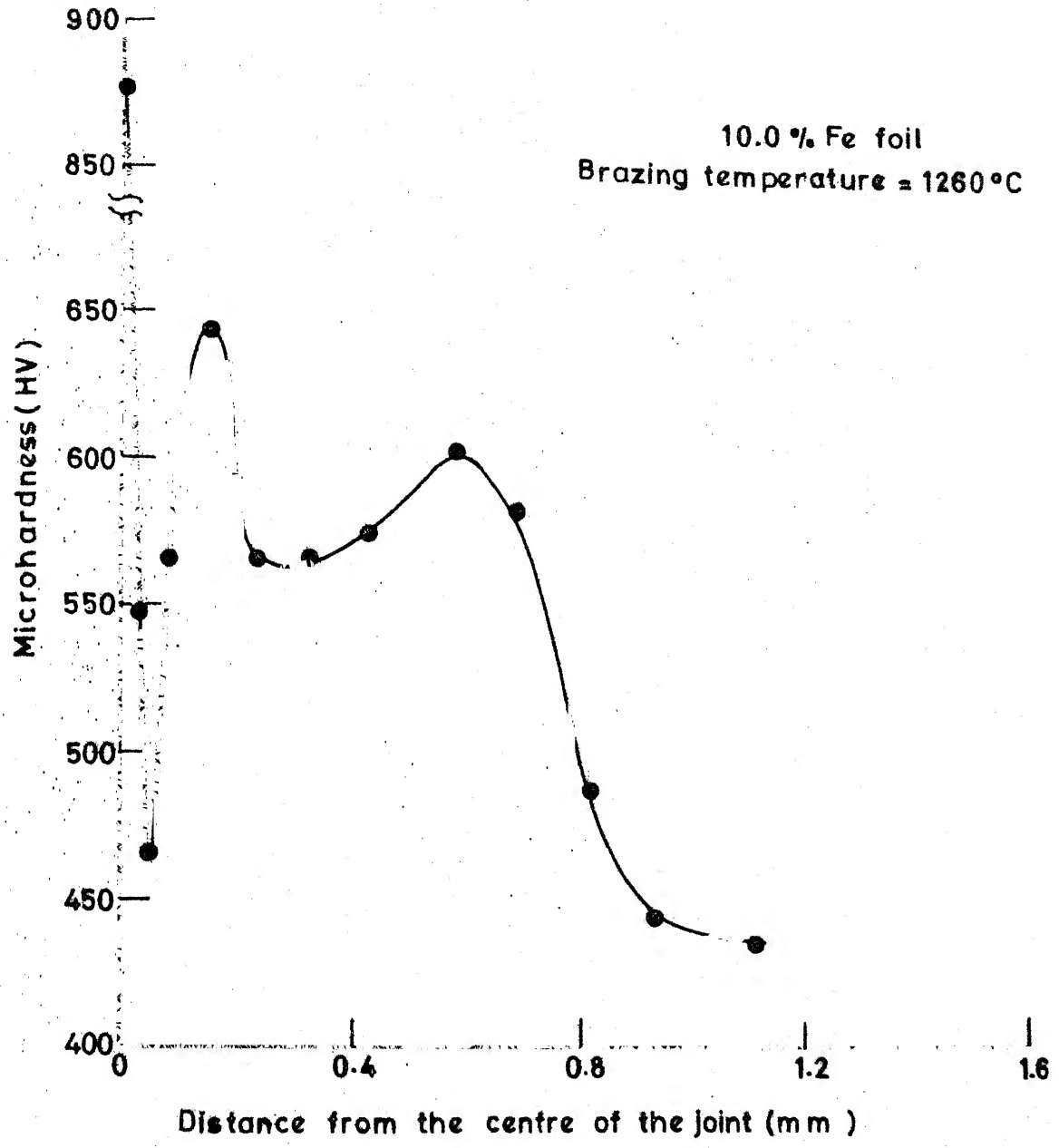

Fig. III.19 Microhardness profile across the brazed section (Alloy III, 1260°C, 600 Sec.)

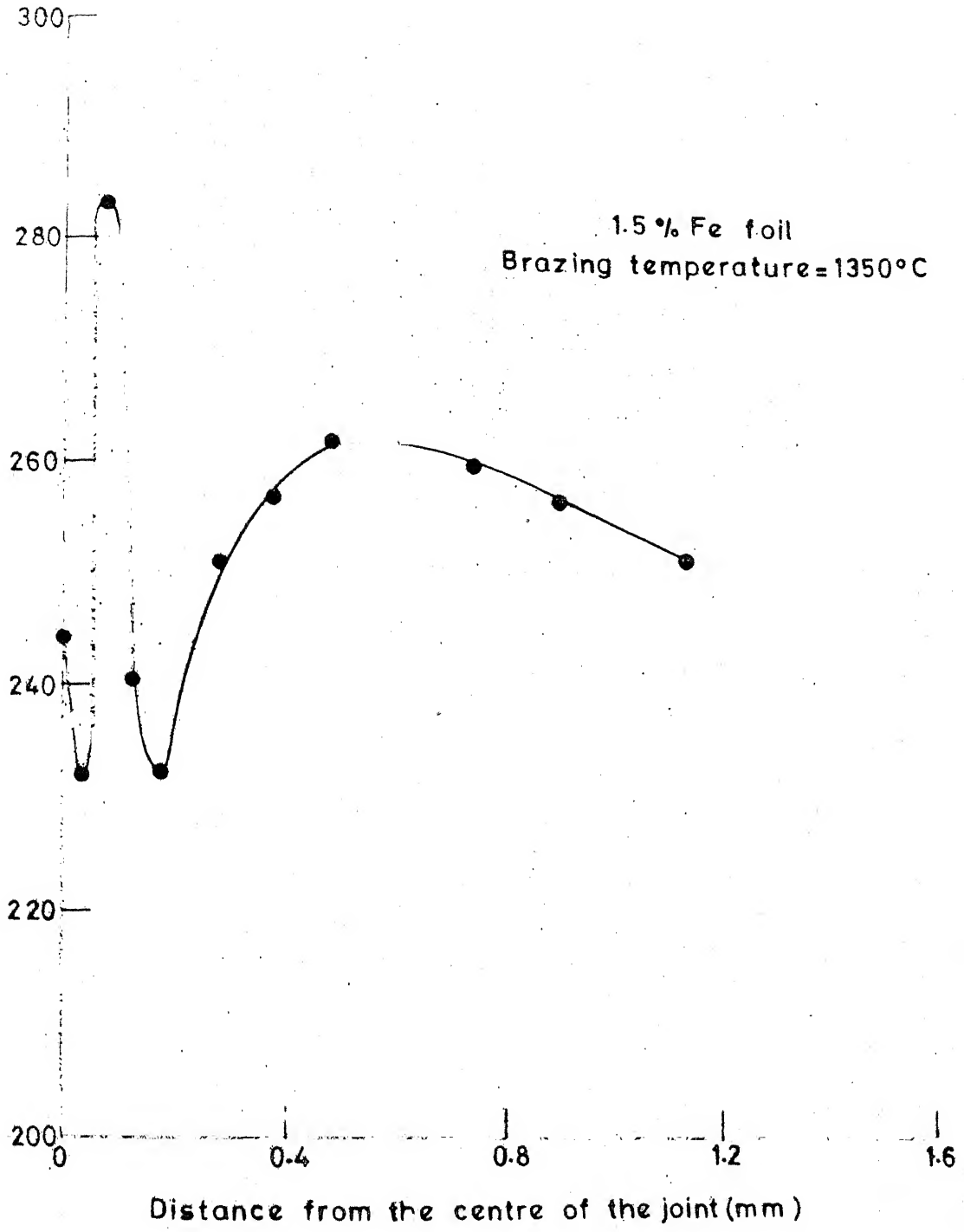

Fig. III.20 Microhardness profile across the brazed section (Alloy I, 1350°C, 600 Sec.)

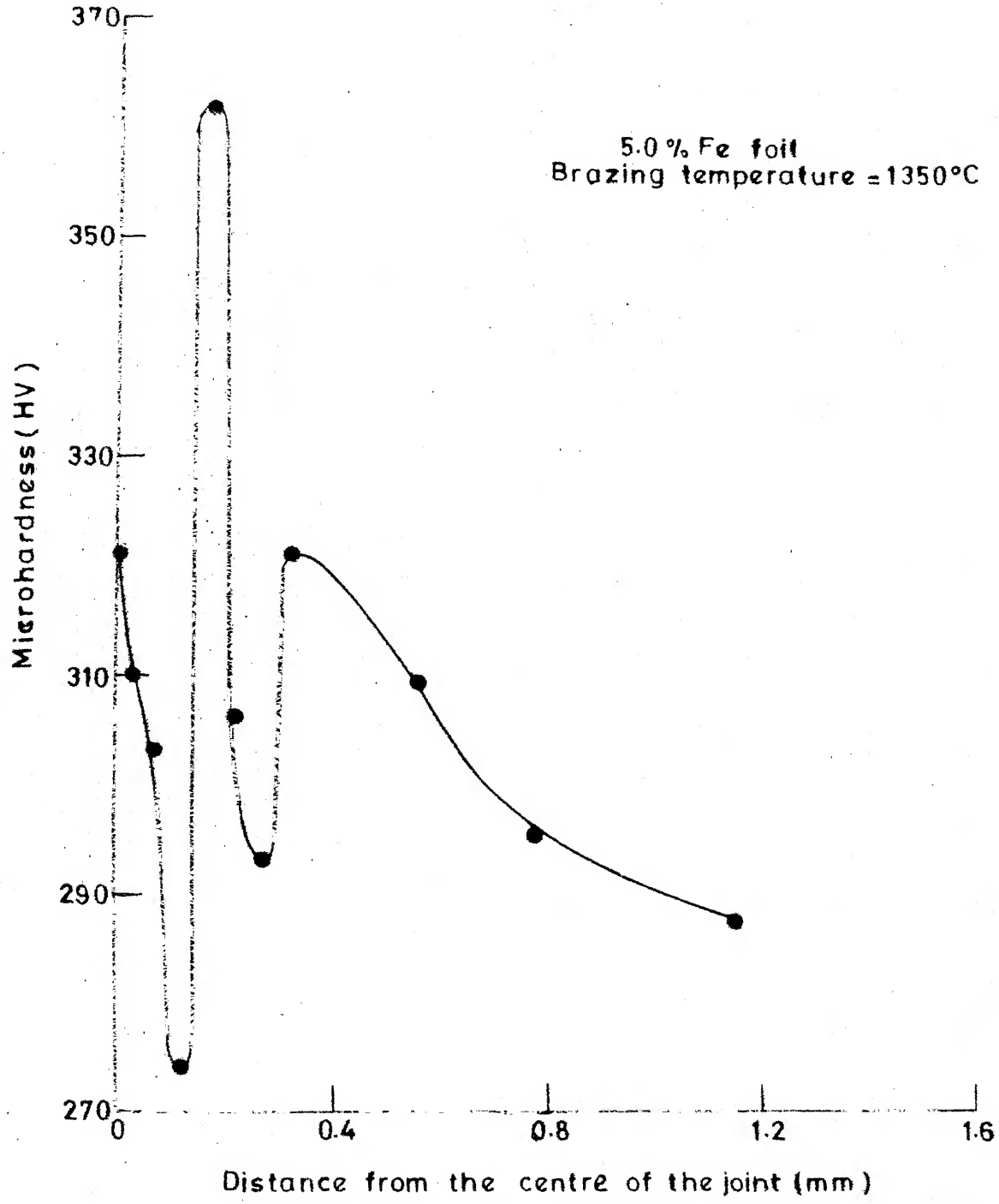

Fig. III.21 Microhardness profile across the brazed section (Alloy II, 1350°C, 600 Sec.)

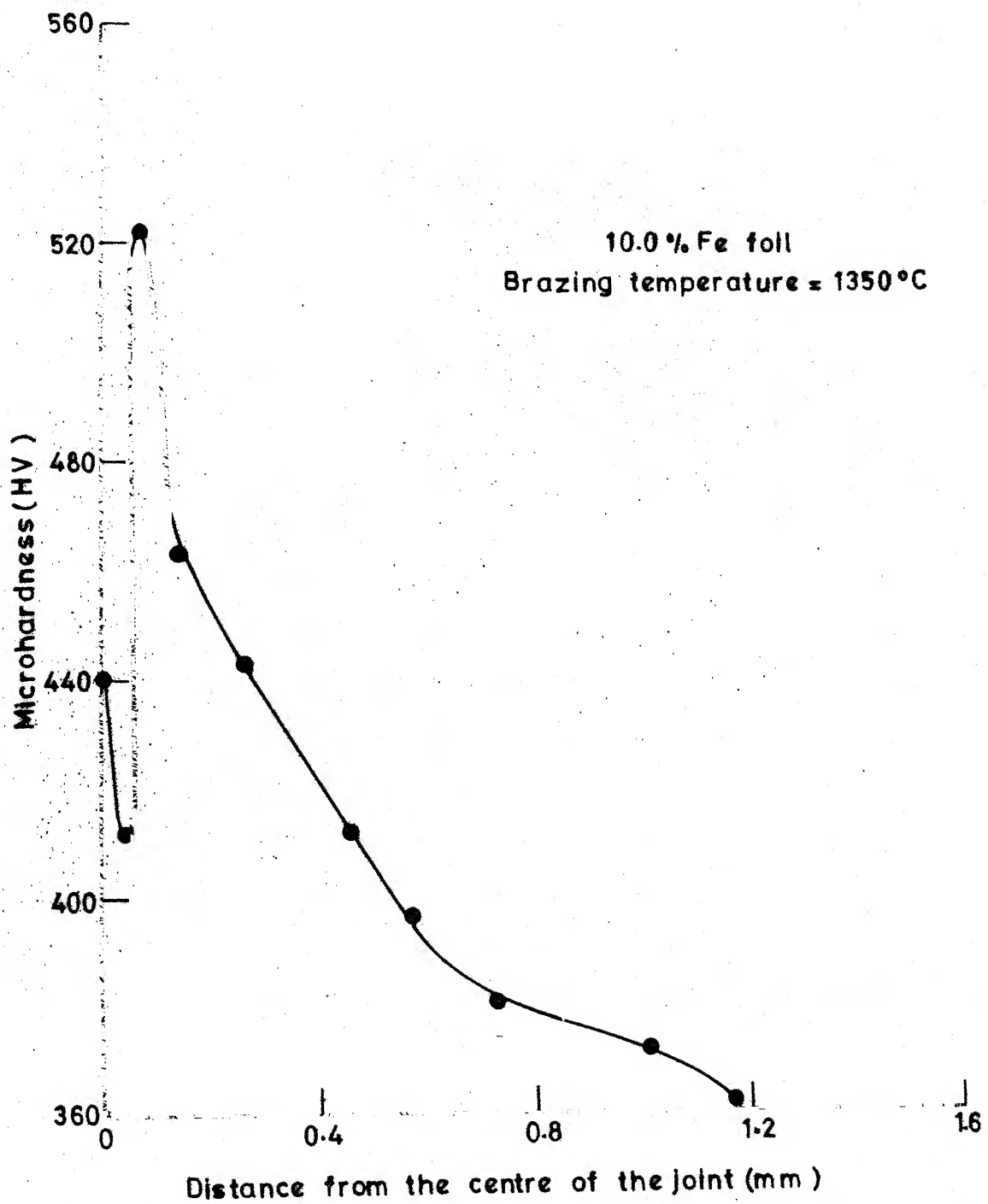

Fig. III.22 Microhardness profile across the brazed section (Alloy III, 1350°C, 600 Sec.)

CHAPTER IV

SUMMARY

Techniques were developed to fabricate ribbons of widths upto 12.5 mm by single roller chill block melt spinning. Continuous and 100 pct. dense aluminium ribbon were obtained by this method but when tried with nickel based alloys, wide ribbons with fine holes were obtained and fully dense ribbon casting trials were not successful because of experimental limitation with the set-up.

X-Ray diffraction pattern revealed the amorphous nature of the nickel based foils and also the vein structure in the fracture surface characterstic of the amorphous phase was obtained.

Two halves of the tensile test specimens of 304 stainless steel was brazed using these foils by resistive heating in a vacuum of 2×10^{-5} torr. The joints had maximum UTS for brazing foils with maximum iron content (average value 348.7 MPa), but the ductility was found to be maximum for the joints brazed with foils containing least iron (average value 6.8 pct. elongation). The strength value is comparable with the values reported in literature for joints brazed with nickel based metallic glass foils.

The metallurgical structures of the joint sections brazed at different temperatures (1260°C and 1350°C) for the same time (600 Sec.) are found to be vastly different. The width of the brazed zone increases with the increasing iron content in the brazing foil.

The microhardness values also undergo large variations as we go from the joint to the base metal matrix, possibly because of the composition variations.

REFERENCE

1. R.W. Cahn, Contemp. Phys., 21, 43 (1980)
2. S.J. Takayama, J. Mater. Sci., 11, 164 (1976)
3. H.S. Chen, H.J. Leamy and C.E. Miller, A Rev. Mater. Sci., 10 , 363 (1980)
4. H.S. Chen, Rep. Prog. Phys., 43 , 353 (1980)
5. B. Leontie, 'Proc. Conf. Amorphous Metallic Materials, Smolenice, 1978,' Eds. P. Duhap and P. Mrafko, p 225, Veda, Bratislava, Yugoslavia (1980)
6. E.H. Strange and C.A. Pim, U.S.P., 905,758, Dec. 1(1980)
7. H.S. Chen and C.E. Miller, Mat.Res. Bull., 11 , 49(1976)
8. K. Klement, R.H. Willens and P. Duwez, Nature, 187, 869 (1960)
9. H.S. Chen, Mater. Sci. Engg., 25, 59 (1976)
10. D.E. Polk and C.A. Pampillo, Scripta Met., 7 , 1161(1973)
11. M. Naka, K. Hashimoto, A. Inoue and T. Masumoto, J. Non-Cryst. Solids, 31, 347 (1979)
12. M. Naka, K. Asami, K. Hashimoto and T. Masumoto, Proc. 4th Int. Conf. Rapidly Quenched Metals, p.449, The Metals Society, London, (1978)
13. N. De Cristofaro and C. Henschel, Welding Journal, 57,(7) 33 (1978)
14. H.E. Pattee, Mach. Design, 41,(21), 111 (1969)
15. R.N. Stenerson, Welding Journal, 48,(6),480 (1969)
16. D. Bose, A. Dutta and N. De Cristofaro, Welding Journal, 60, (10), 29 (1981)

17. G.G.M. Nickel Topics, 35, (1), 9 (1982)

18. G.P.K. Welding Journal, 60,(10), 41 (1981)

19. P. Dewez, Progress in Solid State Chemistry, Vol.3, ed. H. Reiss, p 377 - 406, 1966, Oxford, Pergamon Pres

20. T.R. Anantharam and C. Suryanarayana, J. Mater. Sci., 6, 1111, (1971)

21. H. Jones, Rep. Prog. Phys., 36, 1425 (1973)

22. D. Turnbull, Contemp. Phys., 10, 473 (1969)

23. H.A. Davies, Phys. Chem. Glasses, 17, 159 (1976)

24. F. Spaepen and D. Turnbull, ''Proc. 2nd Internat.Conf. Rapidly Quenched Metals, Sec 1'', ed N.J. Grant and B.C. Giessen, p 205 - 229, 1976, Cambridge, Mass,M.I.T. Press

25. B.G. Lewis and H.A. Davies, Inst. Phys. Conf., Ser.No.3('Liquid Metals', ed R. Evans and D.A. Greenwood, p 274 - 282, 1977, London Inst. of Physics

26. R.B. Pond, U.S. Patent No. 2826108, (March 4), 1958

27. H. Hillman and H.R. Hilzinger, '3rd Conf. Rapidly Quenched Metals,Vol. 1' Sussex, Brighton, p 22, 1978

28. H.H. Liebermann, Mater. Sci. Engg., 43, 203 (1980)

29. S.J.B. Carter, D.R. Mooney, R. Cheese and B. Cantor, J. Mater. Sci., 15, 2658 (1980)

30. S. Kavesh, 'Metallic Glasses', ASM, Metal Park, Ohio (1

31. J.H. Vincent, J.G. Herbertson and H.A. Davies, 'Proc. 4 Rapidly Quenched Metals, Vol.1, Sendai', p 77 - 80,1981

32. P.H. Shingu, K.Kobayashi, R. Suzuki and K. Takeshita, Ref. 31, p 57

33. D. Pavuna, J. Mater. Sci., 16, 2419 (1981)

34. S.C. Huang, Ref. 31, p 65

35. H.H. Liebermann and C.D. Graham, IEEE Trans. on Mag., May, 921, 1976

36. M.C. Narashimhan, U.S. Patent, 4, 142, 571 (1979)

37. S. Takayama and T.Oi, J. Appl. Phys., 50, 96 (1979)

38. H.H. Liebermann, IEEE Trans. Magn., MAG-15, 1393(1979)

39. S.C. Huang and H.C. Fiedler, Mater.Sci. Engg., 51, 39 (1981)

40. H.H. Liebermann, ''Amorphous Metallic Alloys'', ed F.E. Luborsky p 37, Butterworths, London

41. E.A. Chakachery, 'Fabrication and Charecterization of Iron-Boron Metallic Glass Ribbon', M.Tech Thesis, I.I.T., Kanpur

42. W. Feduska, Welding Journal, 38 (3), 1225, (1959)

43. E. Lugscheidler, O. Khotek and R.H. Battenfeld,W.J., 319s, Oct. (1976)

44. L.B. Lundberg, W.C. Turner and C.O. Hoffmann, W.J., 311s, Oct.(1976)

45. I. Amato, P.G. Cappelli and G. Fenoglio, W.J.,338s, Oct.(1975)

46. D.E. Schillinger and H.J. Addision (Jr.), W.J.,302s, Oct. (1976)

47. E. Lugscherder and K. Iverson, W.J., 319s, Oct.(1977)

48. S. Lamb and F.M. Miller, W.J., 48(7), 383s, (1969)

49. C.J. Thwaites, 'Capillary Joining-brazing and soft soldering', p 82 - 83, Research Study Press

APPENDIX

SILVER, COPPER, PALLADIUM AND GOLD BASED BRAZING FILLER METALS USED FOR STAINLESS STEEL BRAZING

AWS - ASTM DESIGNATION	MELTING TEMPERATURE (°C)		BRAZING TEMPERATURE (°C)	NOMINAL COMPOSITION wt.pct.
	SOLIDUS	LIQUIDUS		
SILVER ALLOYS				
BAg-1	606.6	617.7	617.7 - 759.2	45 Ag, 15 Cu, 16 Zn, 24 Cd
BAg-1a	626.0	634.3	684.3 - 759.2	45 Ag, 15.5 Cu, 16.5 Zn, 24 Cd
BAg-2	606.6	700.9	700.9 - 824.5	35 Ag, 26 Cu, 21 Zn, 18 Cd
BAg-3	631.5	687.1	687.1 - 814.7	50 Ag, 15.5 Cu, 15.5 Zn, 16 Cd, 3 Ni
BAg-4	670.4	778.6	778.6 - 870.2	40 Ag, 30 Cu, 28 Zn, 2 Ni
BAg-5	675.9	742.6	742.6 - 824.5	45 Ag, 30 Cu, 25 Zn
BAg-6	687.0	773.1	773.1 - 870.2	50 Ag, 34 Cu, 16 Zn
BAg-7	617.7	651.0	651.0 - 759.2	56 Ag, 22 Cu, 17 Zn, 5 Sn
BAg-8	778.6	778.6	778.6 - 897.9	72 Ag, 28 Cu,
BAg-8a	764.7	764.7	764.7 - 870.2	72 Ag, 28 Cu, 0.2 Ni
BAg-13	717.6	856.3	856.3 - 967.3	54 Ag, 40 Cu, 5 Zn, 1 Ni
BAg-18	601.0	717.6	717.6 - 824.5	60 Ag, 40 Cu

Appendix (Cont.)

ASW - ASTM DESIGNATION	MELTING TEMPERATURE (°C) SOLIDUS	MELTING TEMPERATURE (°C) LIQUIDUS	BRAZING TEMPERATURE (°C)	NOMINAL COMPOSITION wt.pct.
BAg-19	778.6	778.6	778.6 - 1003.4	92 Ag, 8 Cu
COPPER PHOSPHOROUS ALLOYS				
BCuP-1	709.3	897.9	786.9 - 925.7	95 Cu, 5 P
BCuP-2	709.3	792.5	731.5 - 824.5	93 Cu, 7 P
BCuP-3	624.69	806.4	703.7 - 814.7	89 Cu, 5 Ag, 6 P
BCuP-4	624.69	723.1	703.7 - 786.9	87 Cu, 6 Ag, 7 P
BCuP-5	624.69	800.8	703.7 - 814.7	80 Cu, 15 Ag, 5 P
COPPER AND COPPER-ZNIC ALLOYS				
BCu-1	1081.1	1081.1	1092.2 - 1147.7	99.9 Cu (min.)
BCu-1a	1081.1	1081.1	1092.2 - 1147.7	99.0 Cu (min.)
BCu-2	1081.1	1081.1	1092.2 - 1147.7	86.5 Cu (min.)
RBCuZn-A	886.9	897.9	909.1 - 953.5	57 Cu, 42 Zn, 1 Sn
RBCuZn-B	920.2	934.0	936.8 - 981.2	47 Cu, 11 Ni, 42 Zn

(Reference 14)

BS 1845 GRADE	MELTING TEMPERATURE (°C) SOLIDUS	LIQUIDUS	NOMINAL COMPOSITIO wt. pct.
PALLADIUM BEARING ALLOYS			
PD-1	805	810	5 Pd, 68 Ag, 27 Cu
PD-6	900	950	25 Pd, 54 Ag, 21 Cu
PD-7	970	1010	5 Pd, 95 Ag
PD-10	1180	2000	33 Pd, 64 Ag, 3 Mn
PD-11	1120	1120	21 Pd, 31 Mn, 48 Ni
PD-14	1235	1235	60 Pd, 40 Ni
GOLD BASED ALLOYS			
AU-1	905	910	80 Au,19 Cu, 1 Fe
AU-2	930	940	63 Au,37 Cu
AU-3	980	1000	38 Au,62 Cu
AU-5	950	950	82 Au,18 Ni

(Reference 49)